The Abdus Salam
International Centre for Theoretical Physics

United Nations
Educational, Scientific and
Cultural Organization

IAEA
International Atomic Energy Agency

2139-9

School on Synchrotron and Free-Electron-Laser Sources and their Multidisciplinary Applications

26 April - 7 May, 2010

Optics and Holography

D. Attwood
University of California
Berkeley

Optics and Holography

David Attwood

University of California, Berkeley

Available optical techniques for soft x-rays and EUV

- Reflection (glancing incidence or multilayer coatings)

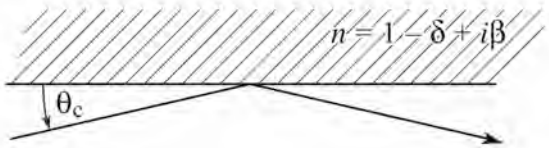

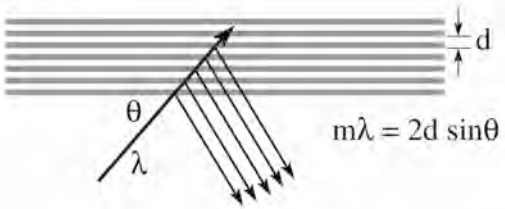

- Diffraction (zone plates, gratings, pinholes)

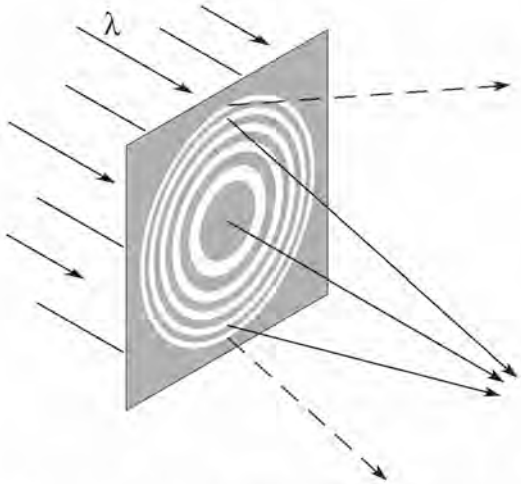

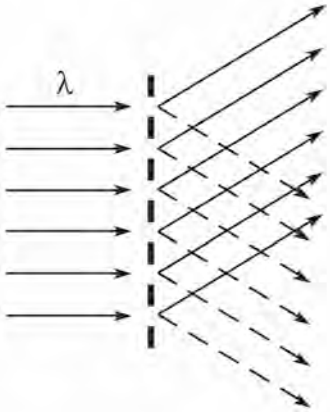

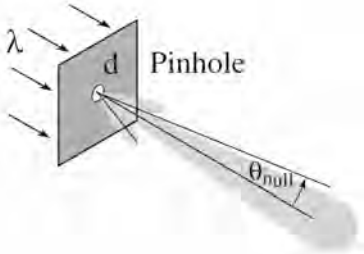

- Refraction (only for hard x-rays, > 20 keV)

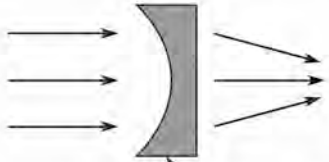

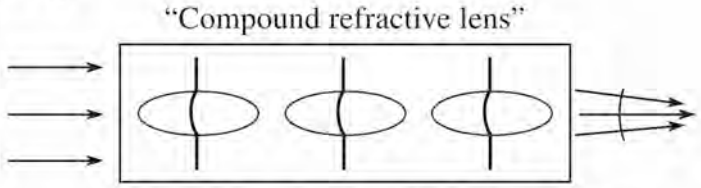

A. Snigerev et al., *Nature* 384, 49 (7Nov.1996)
B. Lengeler et al., *J. Appl. Phys.* 84, 5855 (1Dec.1998)

AvailOpticTechSXREUV.ai

Scattering and refractive index

Refractive Index

$$n = 1 - \delta + i\beta = \frac{n_a r_e \lambda^2}{2\pi}\left(1 - (f_1^0 - i f_2^0)\right)$$

Atomic scattering factor (scattered electric field relative to single free electron)

$f \to f^0$ for $\lambda >> a_0$, or $\theta = 0$ (forward scattering)

Atomic scattering cross-section

$$\sigma = \frac{8\pi}{3} r_e^2 \sum_s \frac{\omega^4}{(\omega^2 - \omega_s^2) - \gamma^2\omega^2} = \frac{8\pi}{3} r_e^2 (f_1^{0\,2} + f_2^{0\,2}) = \frac{8\pi}{3} r_e^2 |f^0|^2$$

Thomson: $\omega^2 >> \omega_s^2$

$$\sigma_T = \frac{8\pi}{3} r_e^2$$

Rayleigh: $\omega^2 << \omega_s^2$

$$\sigma_R = \frac{8\pi}{3} r_e^2 \left[\frac{\lambda_s}{\lambda}\right]^4$$

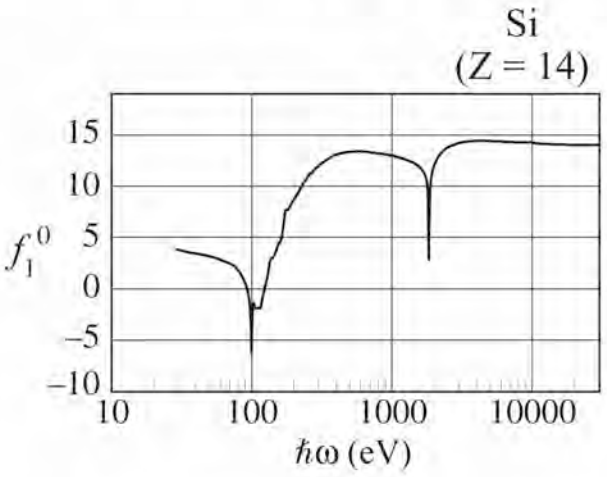

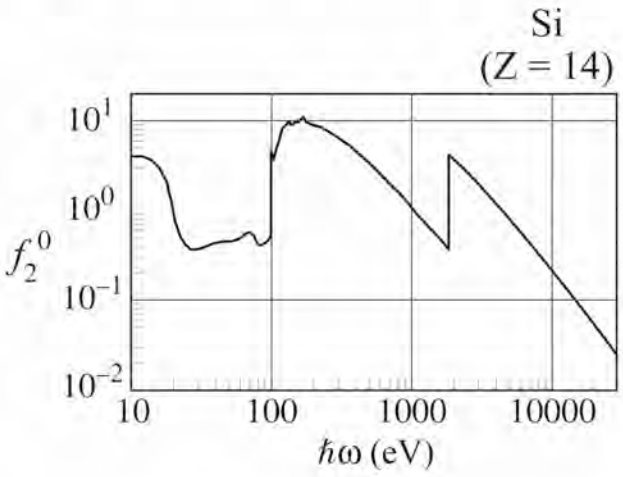

Note:

for $\lambda >> a_0$, and $\omega^2 >> \omega_s^2$

$f_1^0 \to Z$

$f_2^0 \to 0$

ScatrngRefracIndex.ai

Glancing incidence optics

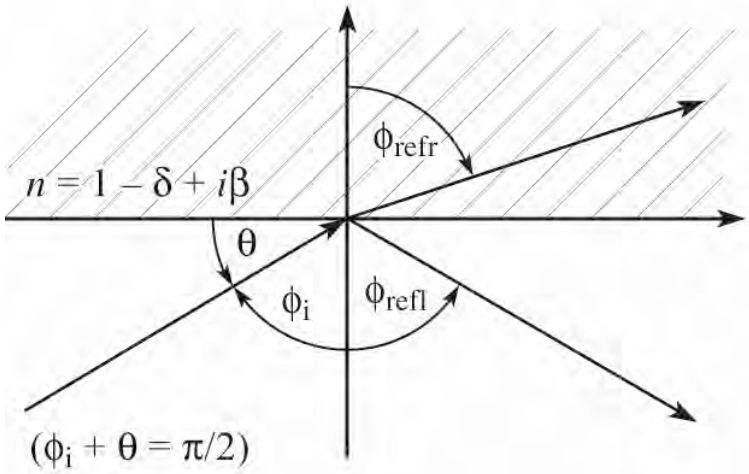

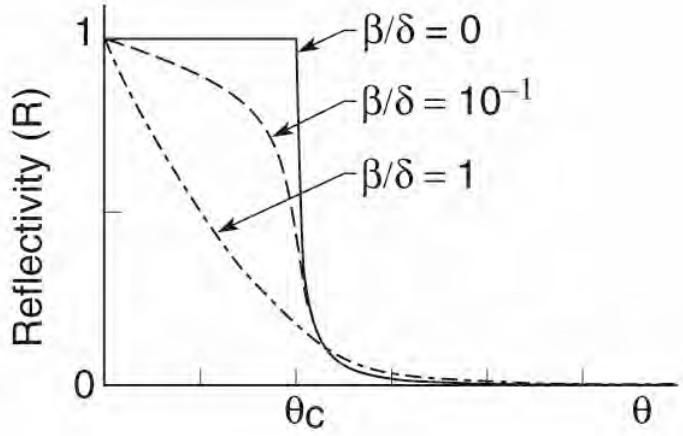

Snell's Law: $\boxed{\text{Sin } \phi_{refr.} = \dfrac{\text{Sin } \phi_i}{n}}$

Total external Reflection:

$$\phi_{refr.} \rightarrow \frac{\pi}{2} \text{ as } \phi_i \rightarrow \phi_{critical}$$

$$\text{Snell's Law: } 1 = \frac{\text{Sin } \phi_c}{1 - \delta}$$

$$\text{Sin}(90° - \theta_c) = 1 - \delta$$

$$\text{Cos } \theta_c = 1 - \delta$$

$$1 - \frac{\theta_c^2}{2} = 1 - \delta$$

$$\theta_c = \sqrt{2\delta}$$

For gold at 1 keV

$$\delta = 2.1 \times 10^{-3}$$

$$\theta_c = 3.7°$$

(www.cxro.LBL.gov ;
"X-ray properties of the elements"
"X-ray interaction with matter")

GlancngIncidncOptics.ai

Scattering by density variations within a multilayer coating

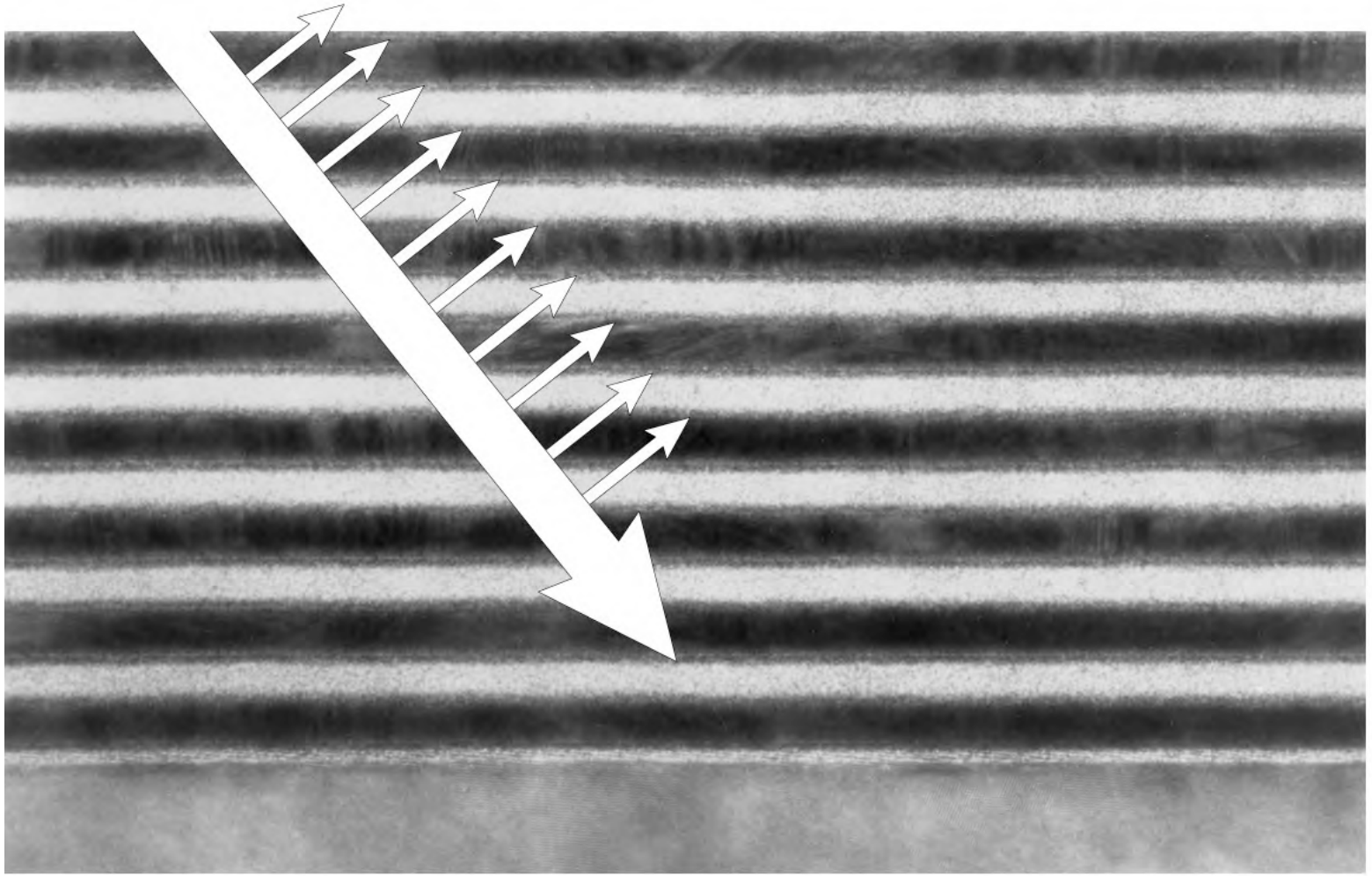

(T. Nguyen, CXRO/LBNL)

Ch04_F01_Feb2007.ai

A high quality Mo/Si multilayer mirror

N = 40
d = 6.7 nm

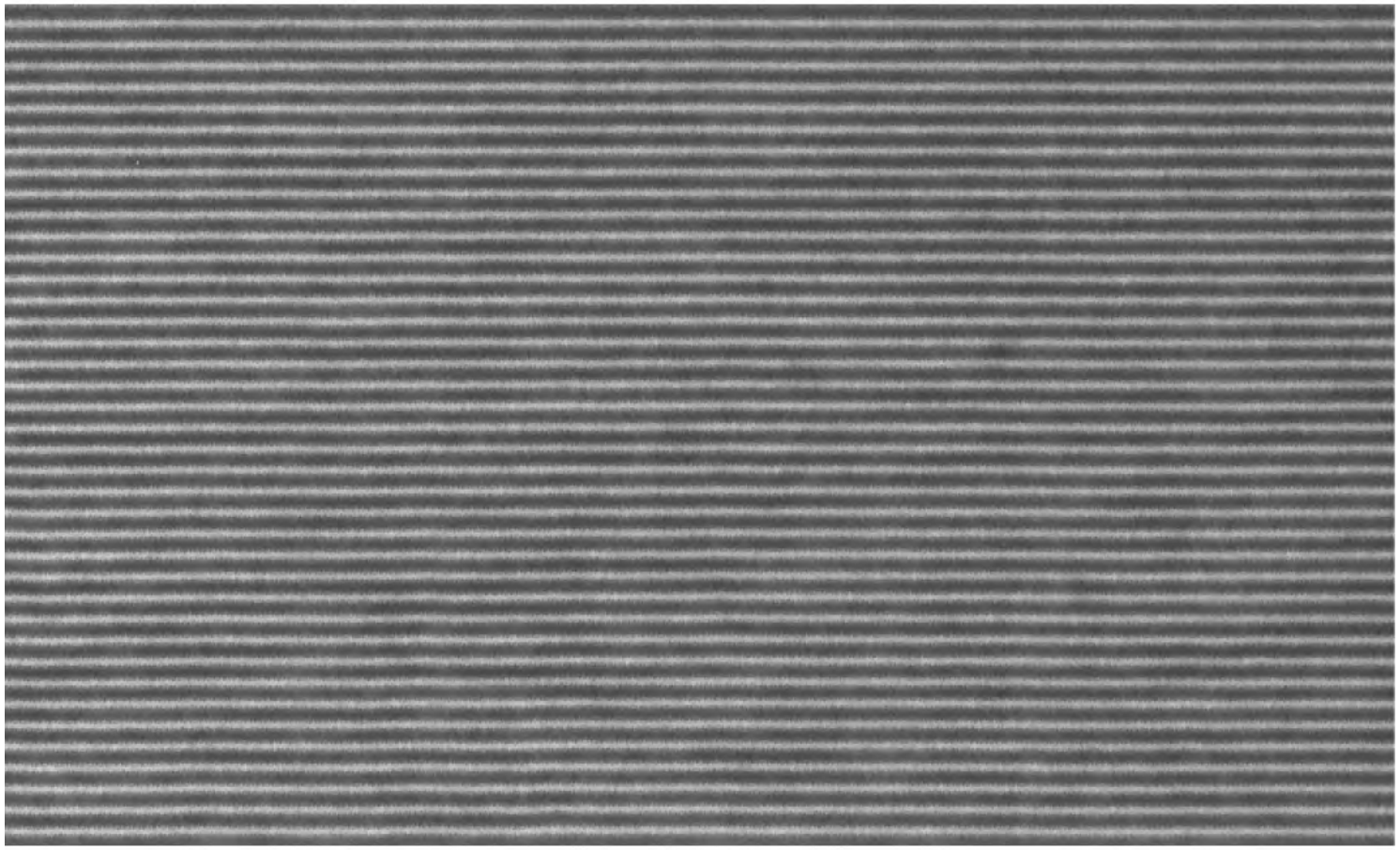

Courtesy of Saša Bajt (LLNL)

Ch04_HiQualtyMoSi.ai

Multilayer mirrors have achieved a reflectivity of 70%

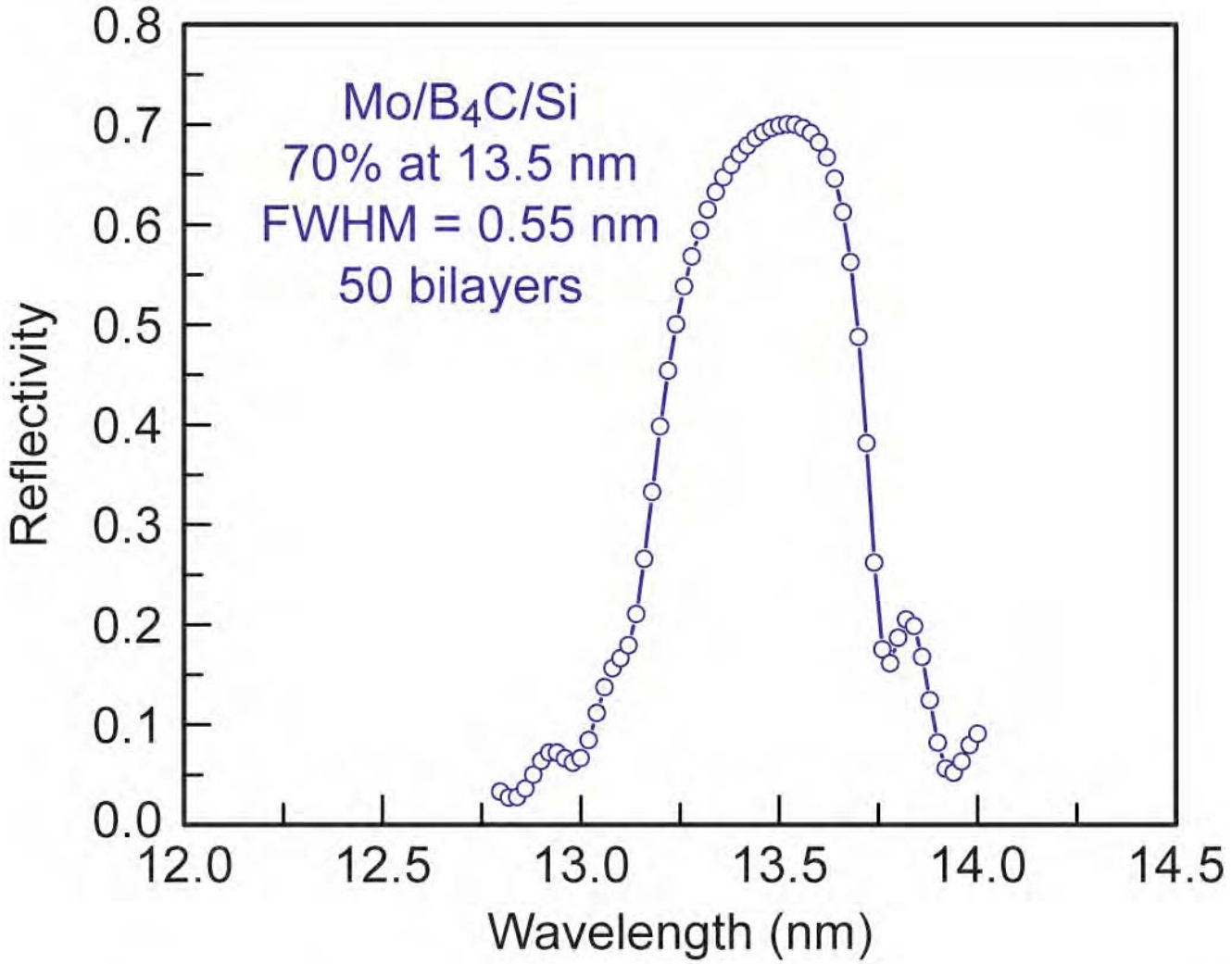

Courtesy of Saša Bajt (LLNL)

Ch04_ReflectCurv70.ai

High reflectivity, thermally and environmentally robust multilayer coatings for high throughput EUV lithography

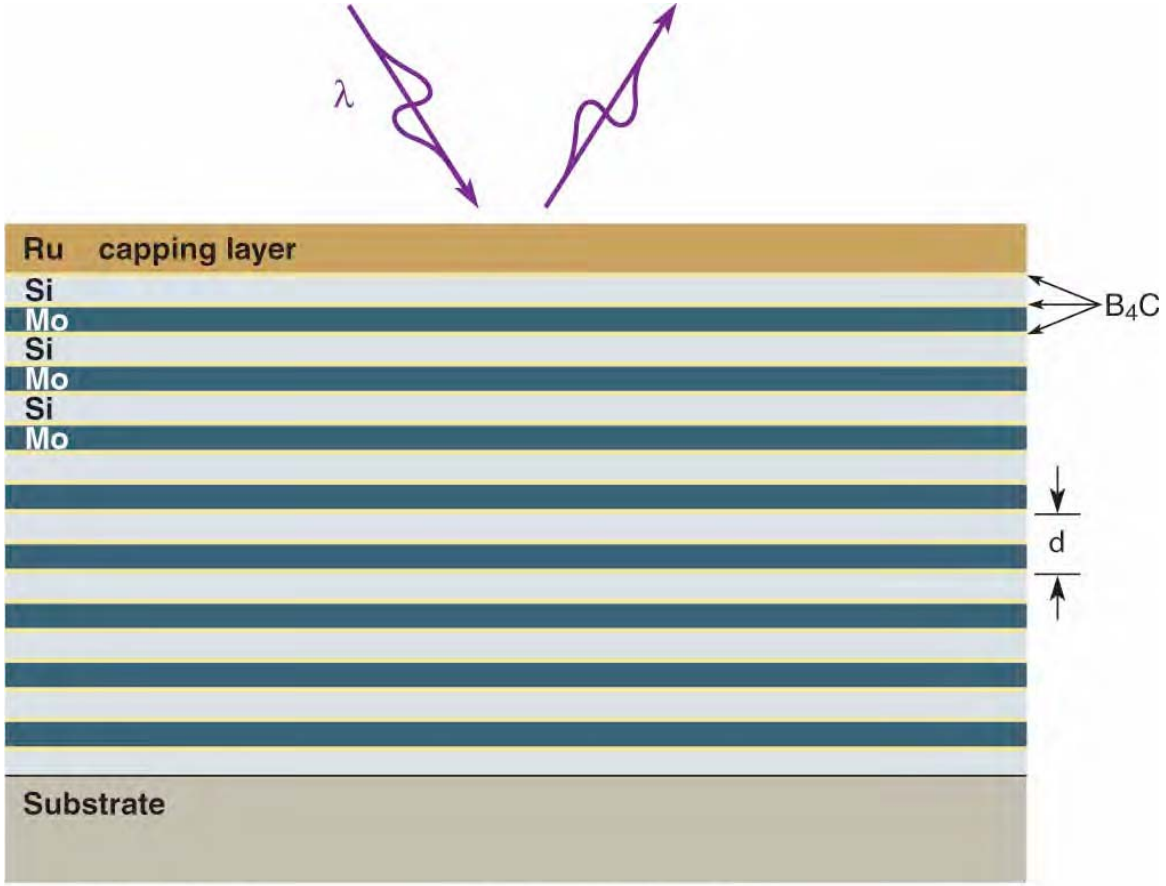

λ = 13.4 nm

Ru (1.70 nm)
Si (4.14 nm)
B_4C (0.25 nm)
Mo (2.09 nm)
B_4C (0.40 nm)

d = 6.88 nm
Γ = 0.34

Courtesy of Saša Bajt (LLNL)

Scattering of radiation by a sinusoidal density distribution (atoms or electrons)

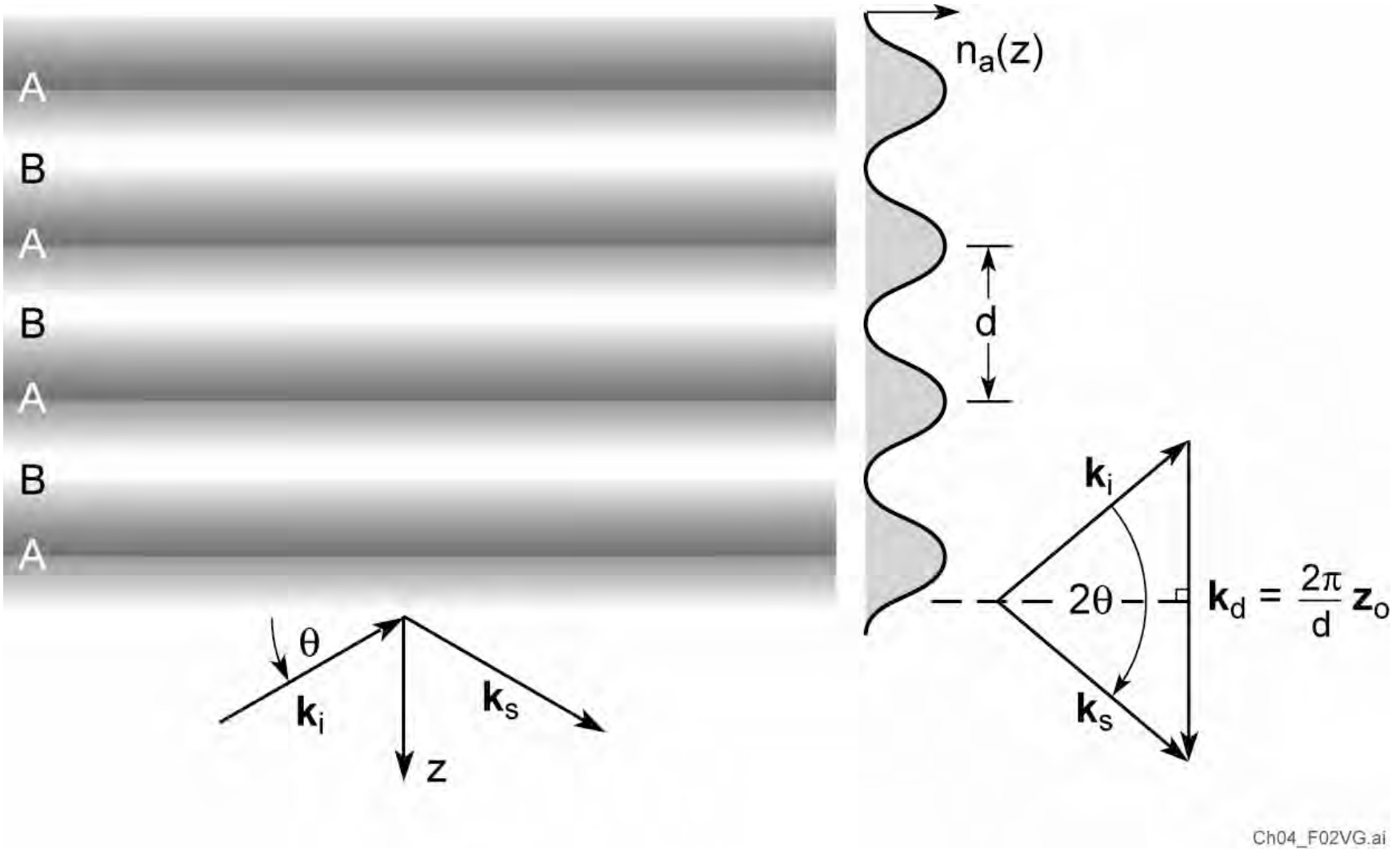

High reflectivity multilayer coatings require:

- Refractive index contrast at the interfaces
- Minimal absorption in the low-Z material
- Thin high-Z layer where possible Γ ; $\Delta\tau_H/(\Delta\tau_H + \Delta\tau_L)$
- Interfaces which are chemically stable with time
- Minimal interdiffusion at the interfaces
- Minimal interfacial roughness (no crystallite formation within the layers, no shadowing in the coating process, surface mobility)
- Thermal stability during illumination
- Chemically stable vacuum interface
  (e.g., $Si0_2$ or capping layer)
- Uniform coating thickness

Atomic scattering factors for silicon (Z = 14)

σ_a(barns/atom) = μ(cm^2/g) × 46.64
E(keV)μ(cm^2/g) = f_2^0 × 1498.22

Silicon (Si)
Z = 14
Atomic weight = 28.086

Energy (eV)	f_1^0	f_2^0	μ(cm^2/g)
30	3.799	3.734E–01	1.865E+04
70	2.448	5.701E–01	1.220E+04
100	–5.657	4.580E+00	6.862E+04
300	12.00	6.439E+00	3.216E+04
700	13.31	1.951E+00	4.175E+03
1000	13.00	1.070E+00	1.602E+03
3000	14.23	1.961E+00	9.792E+02
7000	14.33	4.240E–01	9.075E+01
10000	14.28	2.135E–01	3.199E+01
30000	14.02	2.285E–02	1.141E+00

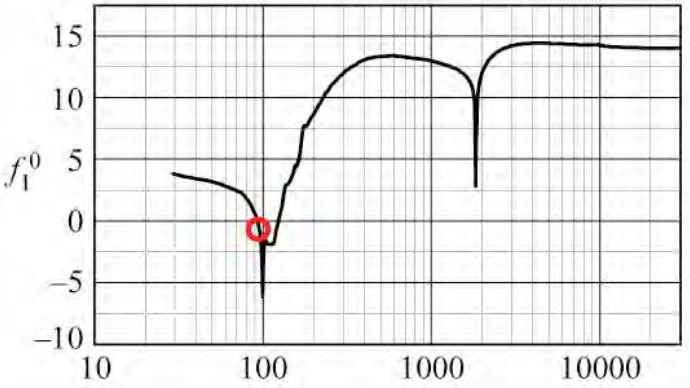

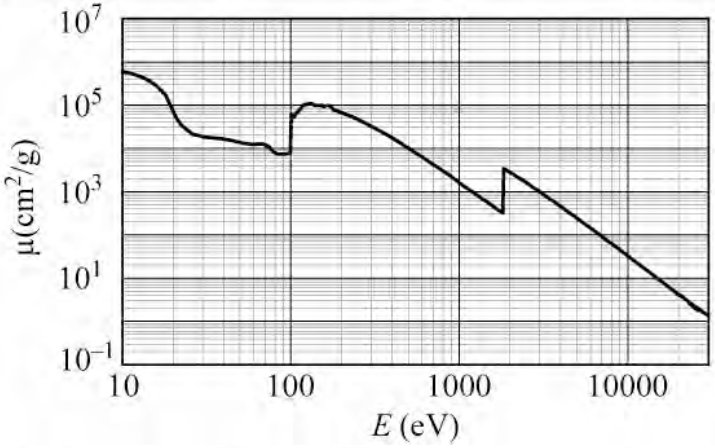

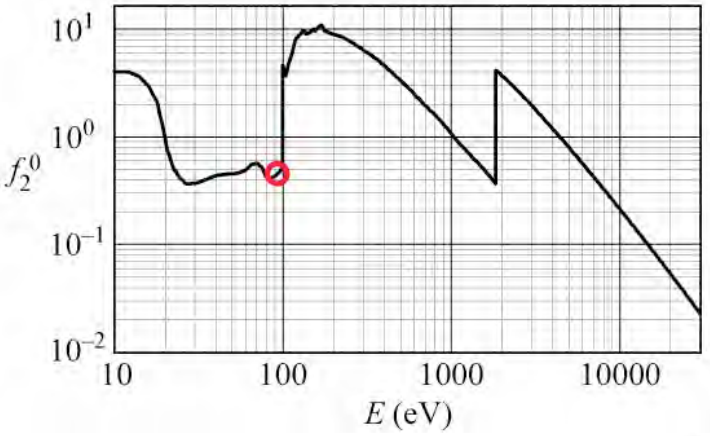

Edge Energies: K 1838.9 eV
L_1 149.7 eV
L_2 99.8 eV
L_3 99.2 eV

(Henke and Gullikson; www-cxro.LBL.gov)

Ch02ApC_Tb1F07_Sept05.ai

Atomic scattering factors for molybdenum (Z = 42)

σ_a(barns/atom) = μ(cm^2/g) × 159.31
E(keV)μ(cm^2/g) = f_2^0 × 438.59

Molybdenum (Mo)
Z = 42
Atomic weight = 95.940

Energy (eV)	f_1^0	f_2^0	μ(cm^2/g)
30	1.071	5.292E+00	7.736E+04
70	19.38	4.732E+00	2.965E+04
100	14.02	1.124E+00	4.931E+03
300	4.609	1.568E+01	2.292E+04
700	31.41	1.819E+01	1.140E+04
1000	35.15	1.188E+01	5.210E+03
3000	35.88	1.366E+01	1.997E+03
7000	42.11	3.493E+00	2.189E+02
10000	41.67	1.881E+00	8.248E+01
30000	42.04	1.894E+00	2.769E+01

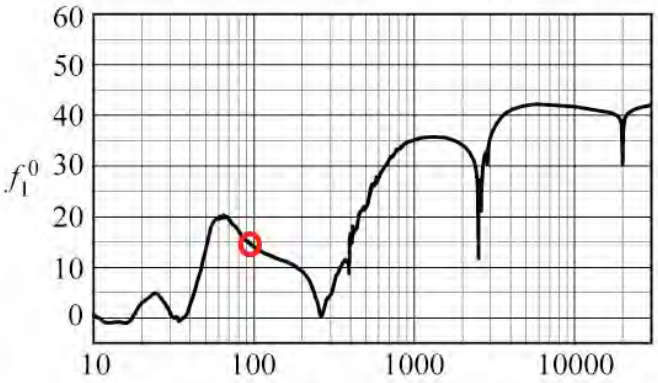

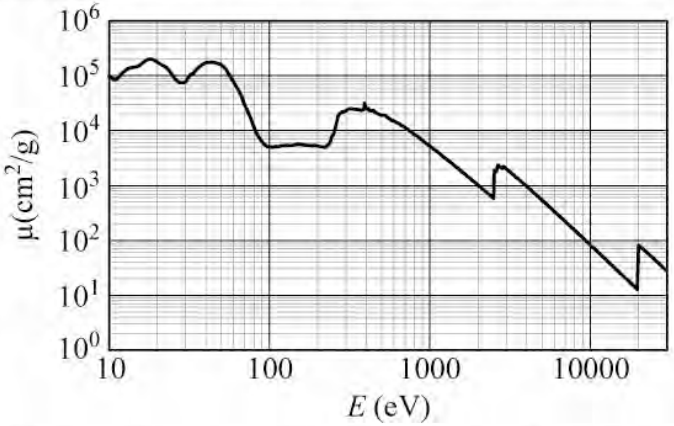

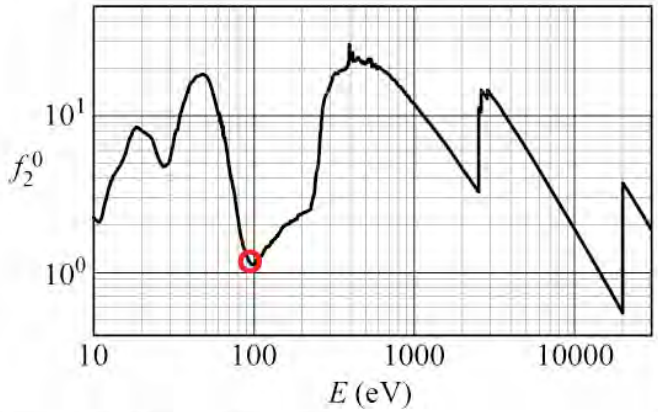

Edge Energies:						
K	19999.5 eV	L_1	2865.5 eV	M_1	506.3 eV	N_1 63.2 eV
		L_2	2625.1 eV	M_2	411.6 eV	N_2 37.6 eV
		L_3	2520.2 eV	M_3	394.0 eV	N_3 35.5 eV
				M_4	231.1 eV	
				M_5	227.9 eV	

(Henke and Gullikson; www-cxro.LBL.gov)

Ch02ApC_Tb1F12_June2008.ai

Multilayer mirrors satisfy the Bragg condition

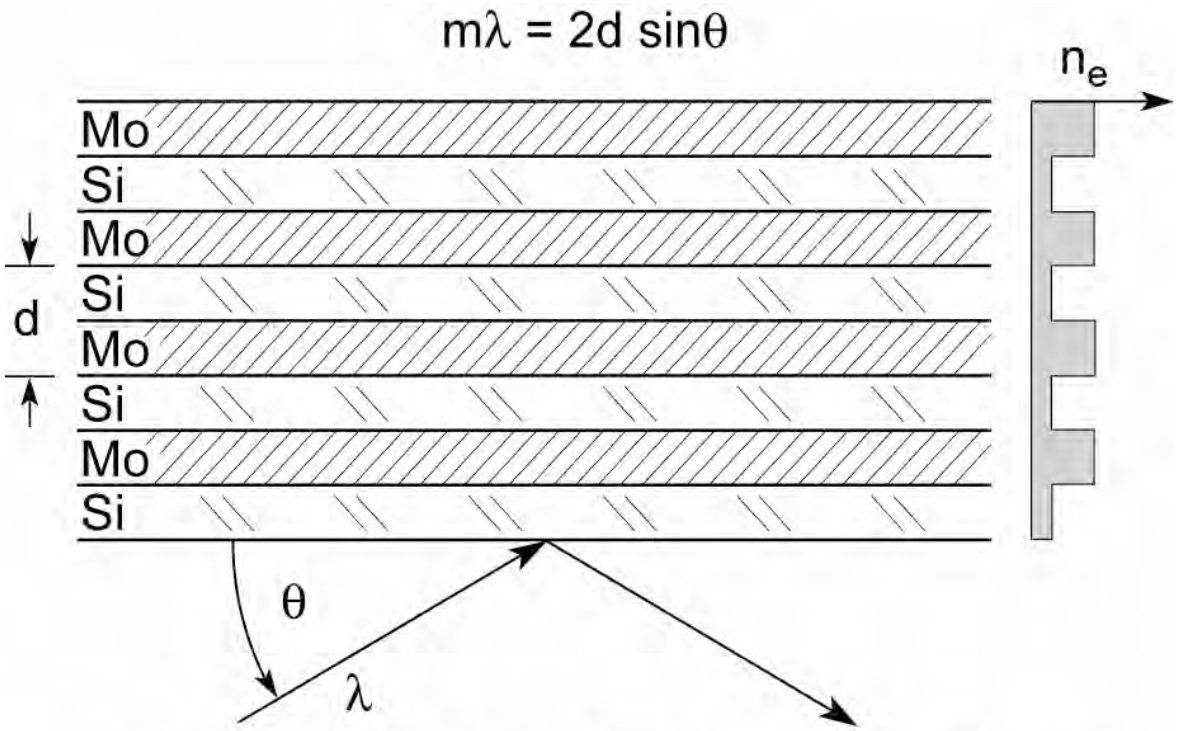

For normal incidence, $\theta = \pi/2$, first order (m = 1) reflection

$$\lambda = 2d$$

$$d = \lambda/2$$

if the two layers are approximately equal

$$\Delta t \simeq \lambda/4$$

a quarter-wave plate coating.

Ch04_MltlyrMirBragg1.ai

Multilayer mirrors satisfy the Bragg condition

$$m\lambda = 2d \sin\theta \left(1 - \frac{4\bar{\delta}d^2}{m^2 \lambda^2}\right)$$

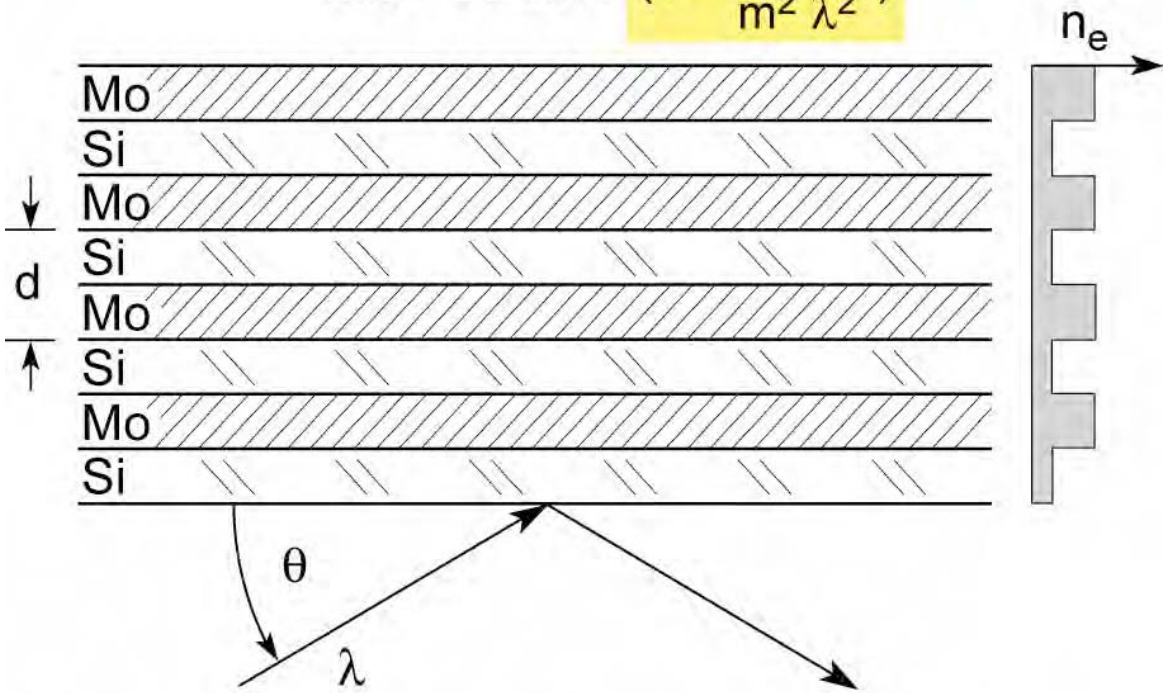

For normal incidence, $\theta = \pi/2$, first order (m = 1) reflection

$$\lambda = 2d$$

$$d = \lambda/2$$

if the two layers are approximately equal

$$\Delta t \simeq \lambda/4$$

a quarter-wave plate coating.

Ch04_MltlyrMirBragg2.ai

Sputtered deposition of a multilayer coating

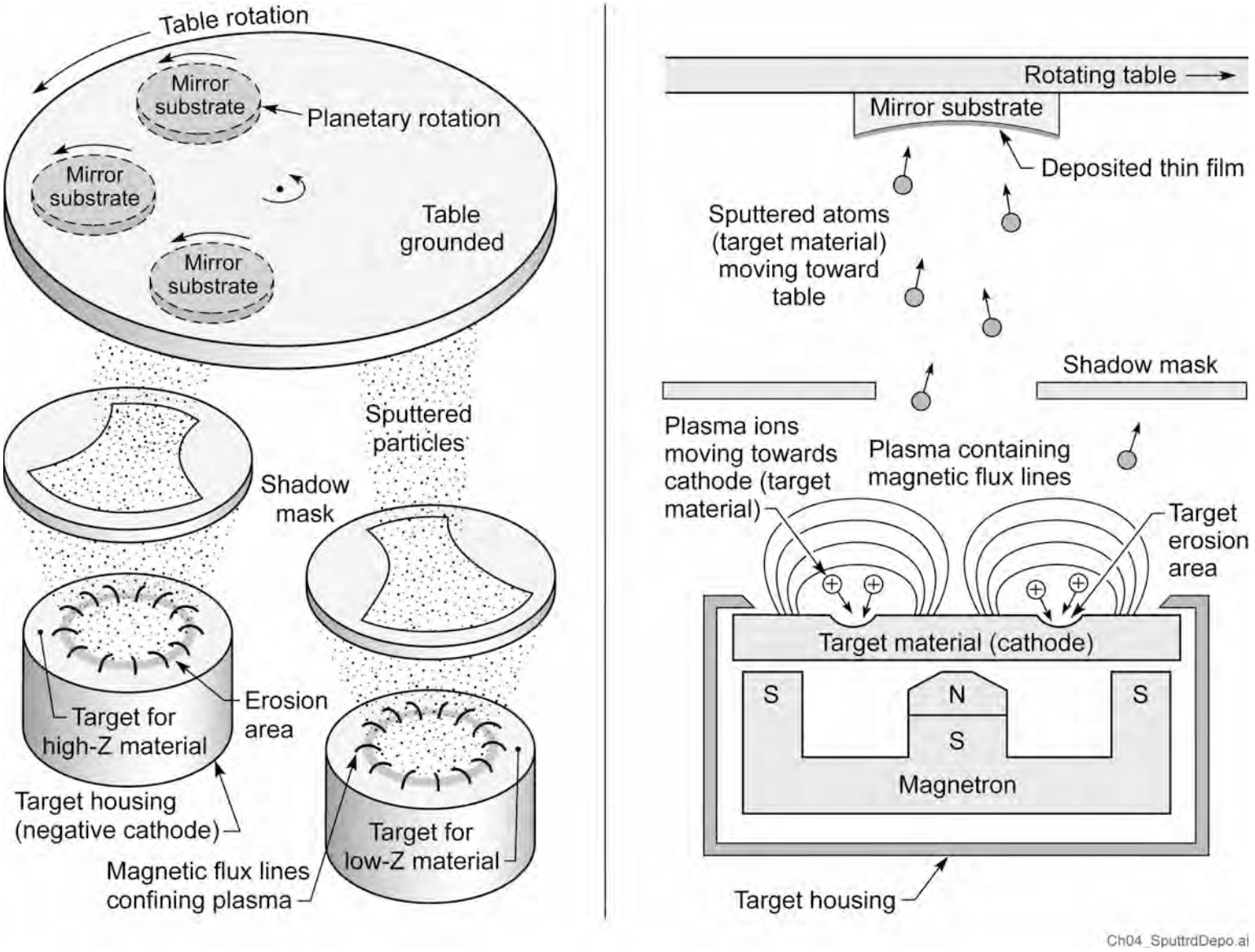

Fluorescent microprobe based on crossed cylinders and multilayer coatings

Kirkpatrick-Baez (KB) optics

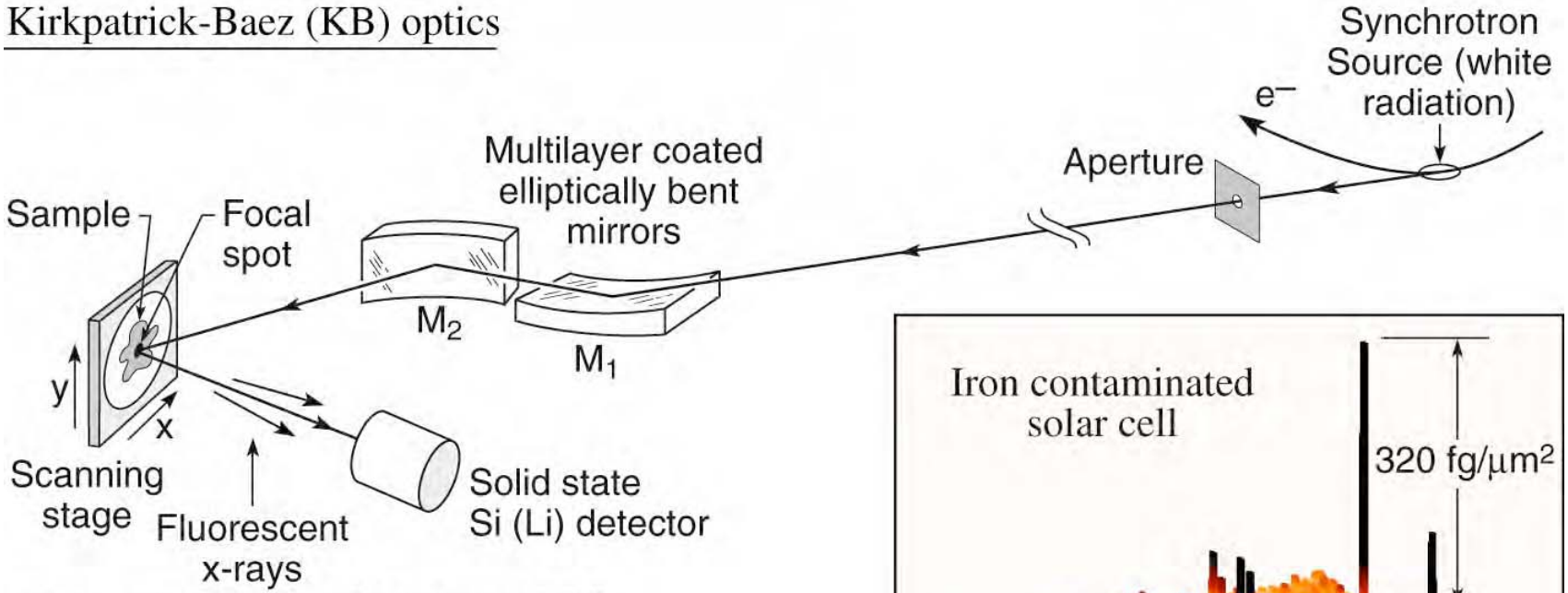

(Courtesy of A. Thompson and J. Underwood, LBNL; and R. Holm, Miles Lab)

- Crossed cylinders at glancing incidence
- Ellipses better
- Photon in / photon out, low noise background
- Femtogram and part per billion (ppb) sensitivity
- Sub-micron focus (to 0.1 μm recently), but scattering gives several micron "50% encircled energy"
- K-B optics have many applications to synchrotron beamlines, fusion diagnostics, etc.

FluoresMicroprobe.ai

Microprobe analysis of contaminated soil

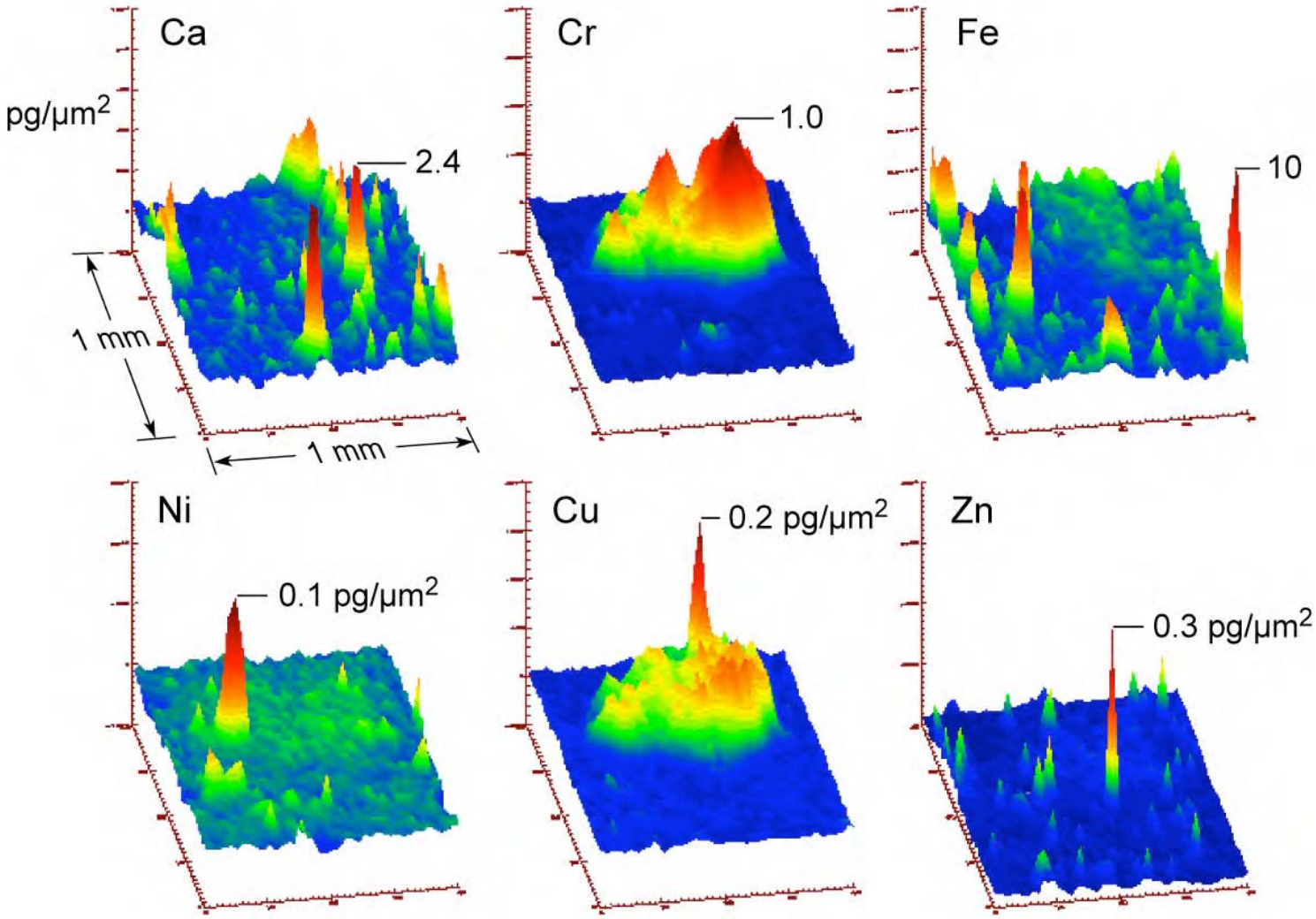

(Courtesy of T. Tokunaga; and A. Thompson, LBNL)

Ch04_F15VG.ai

High resolution x-ray diffraction under high pressure using multilayer coated focusing optics

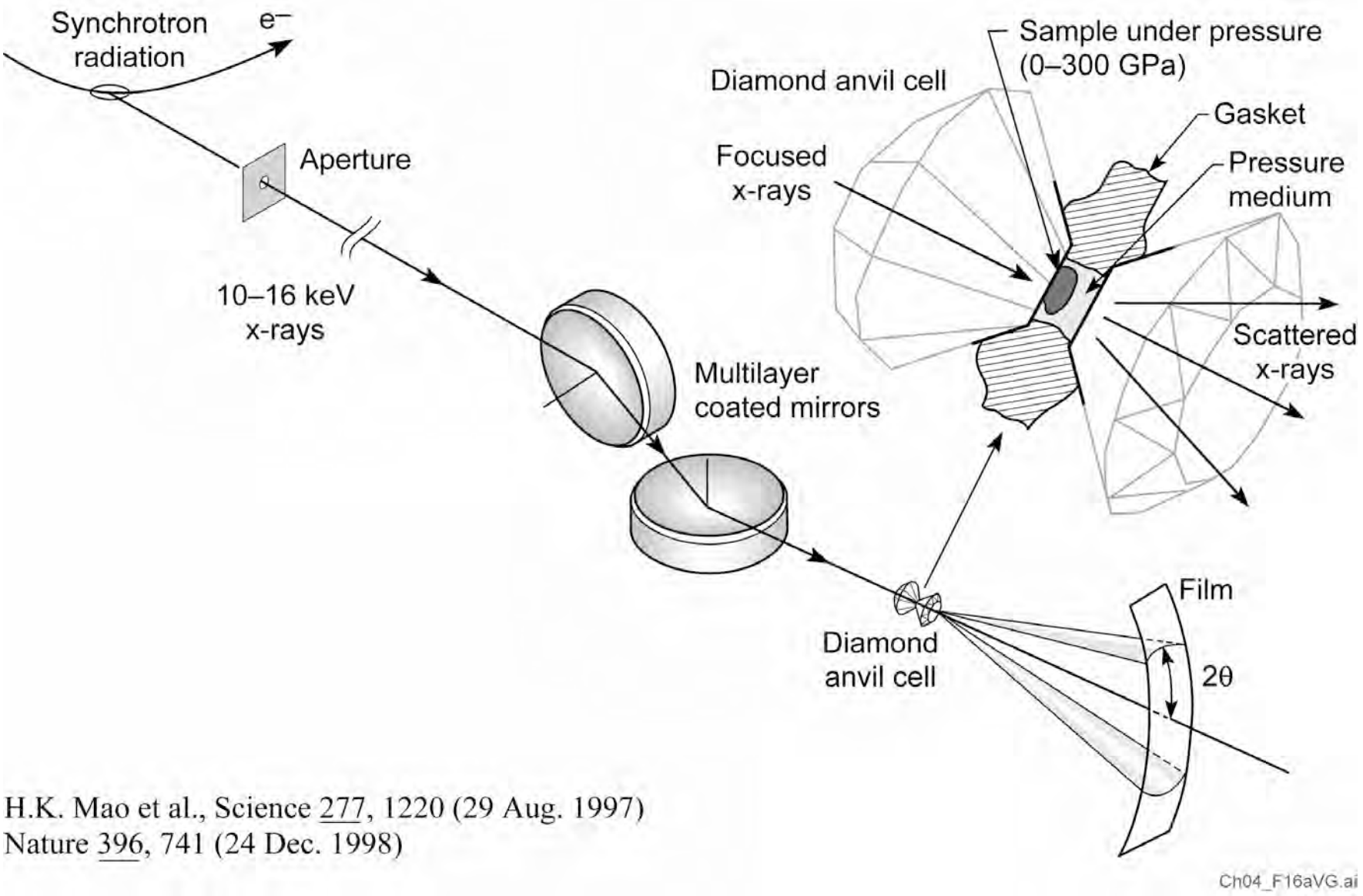

H.K. Mao et al., Science 277, 1220 (29 Aug. 1997)
Nature 396, 741 (24 Dec. 1998)

The Cassegrain telescope

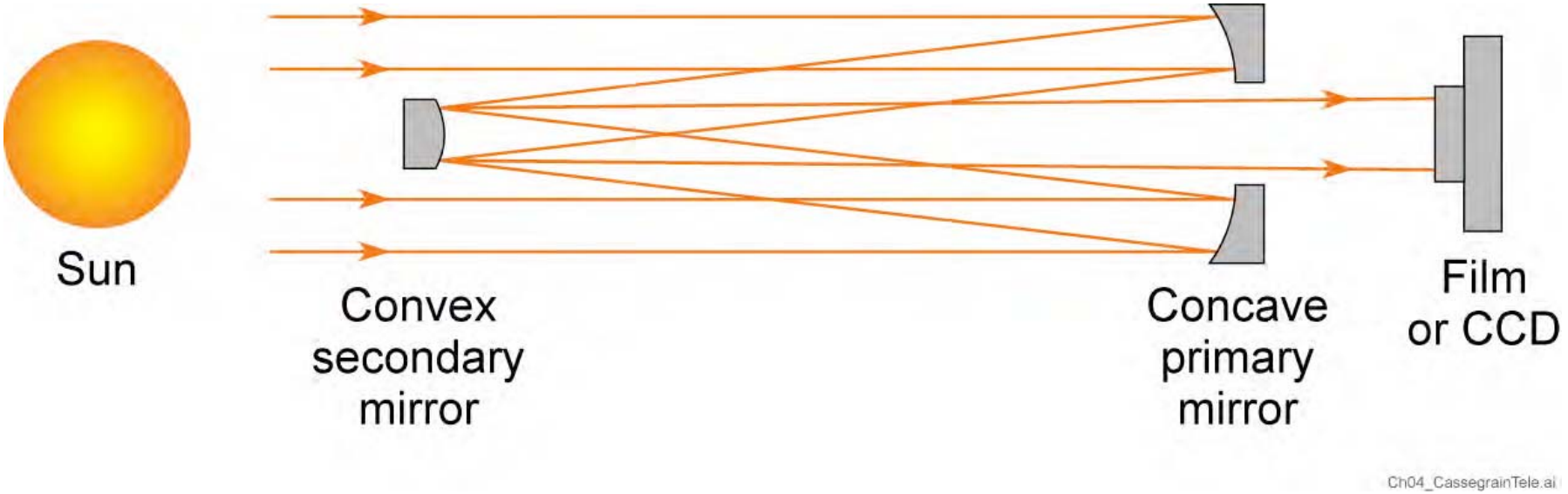

EUV image of the solar corona showing loops near the solar limb

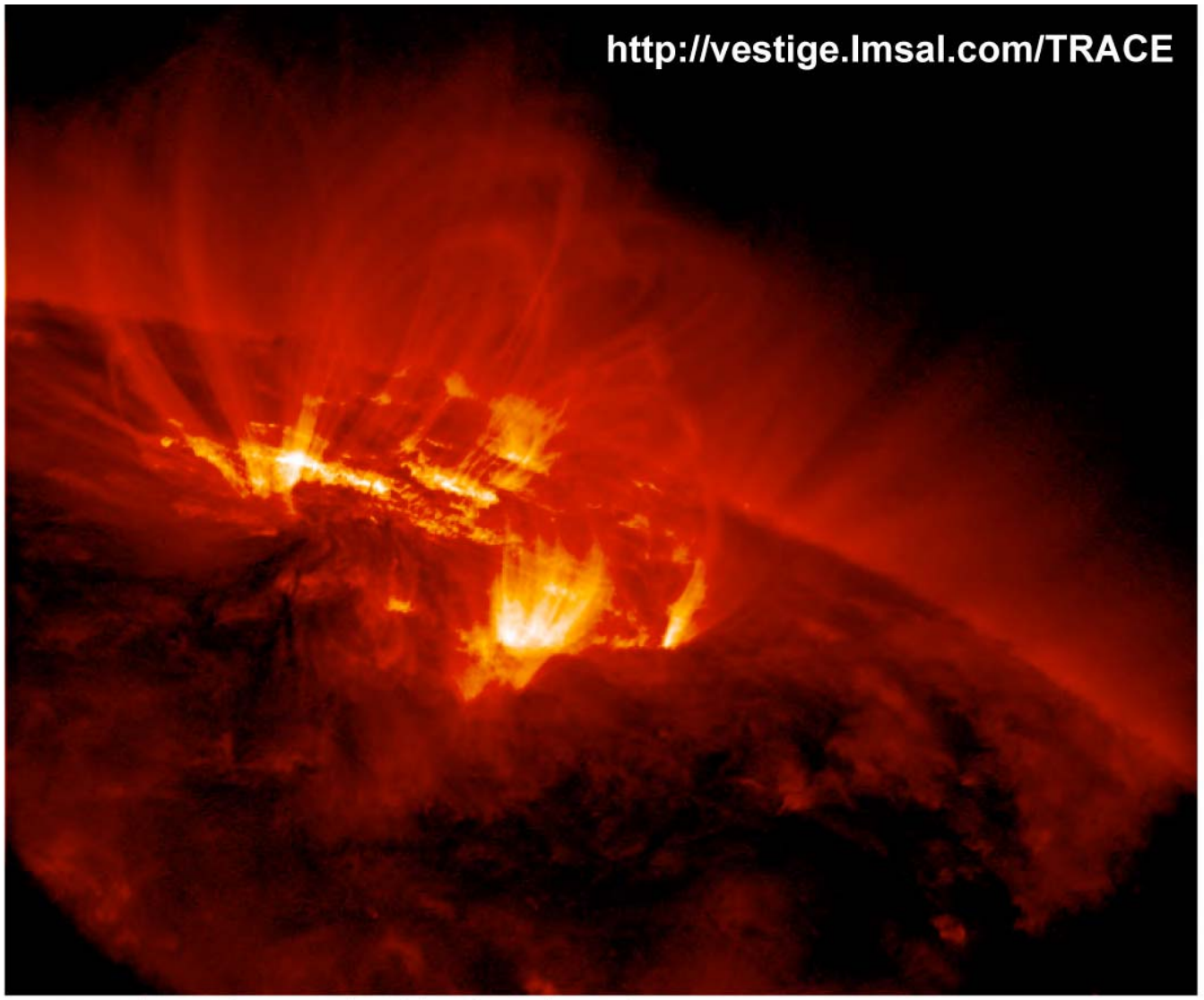

λ = 17.3 nm
(71.7 eV)

(Courtesy of L.Golub, Harvard-Smithsonian and T. Barbee, LLNL)

Ch04_F10VG_Sept05.ai

Diffractive optics for soft x-rays and EUV

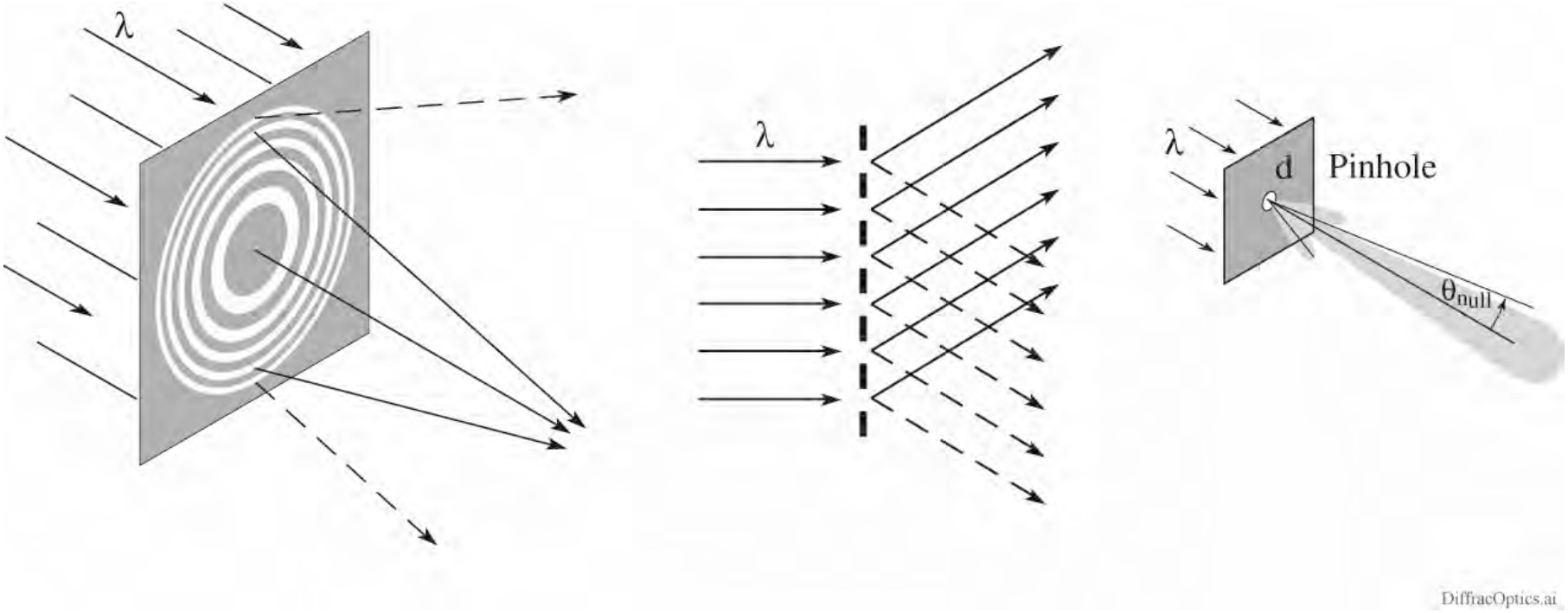

Diffraction from a transmission grating

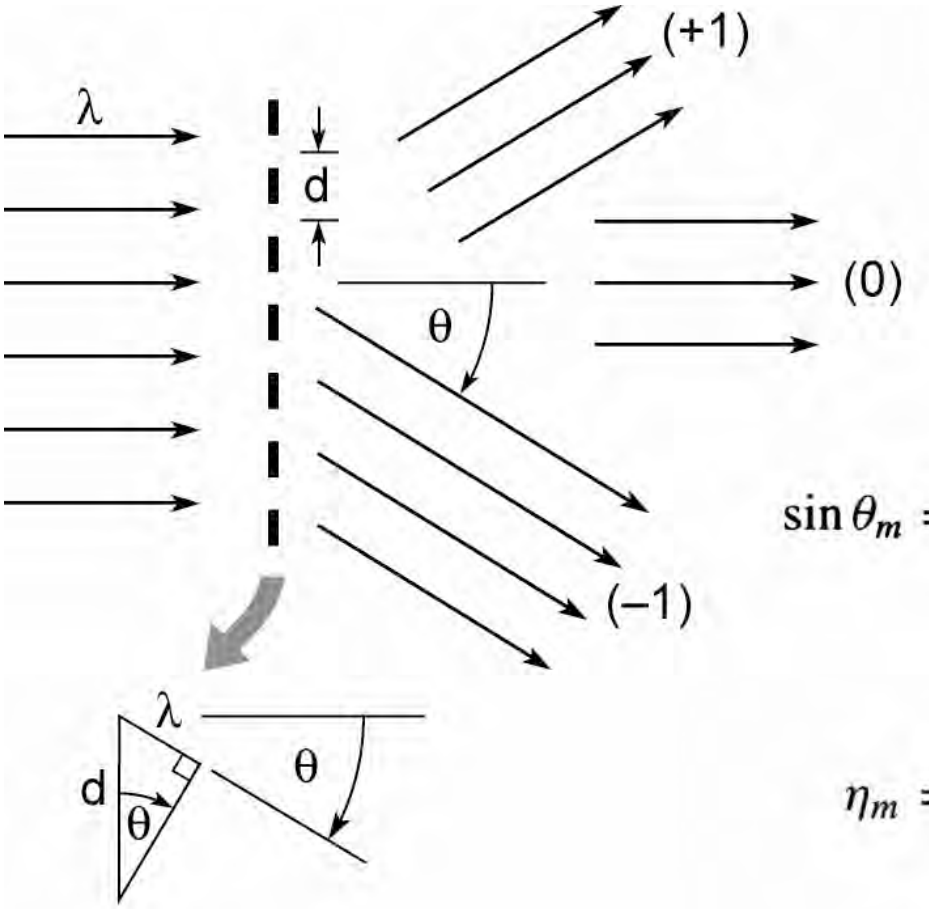

$$\sin\theta_m = \frac{m\lambda}{d}\,; \quad m = 0, \pm 1, \pm 2, \pm 3, \ldots \quad (9.2)$$

$$\eta_m = \begin{cases} \frac{1}{4} & m = 0 \\ 1/m^2\pi^2 & m \text{ odd} \\ 0 & m \text{ even} \end{cases} \quad (9.24)$$

(50% absorbed)

Ch09_F03VGrev4.04.ai

A Fresnel zone plate lens

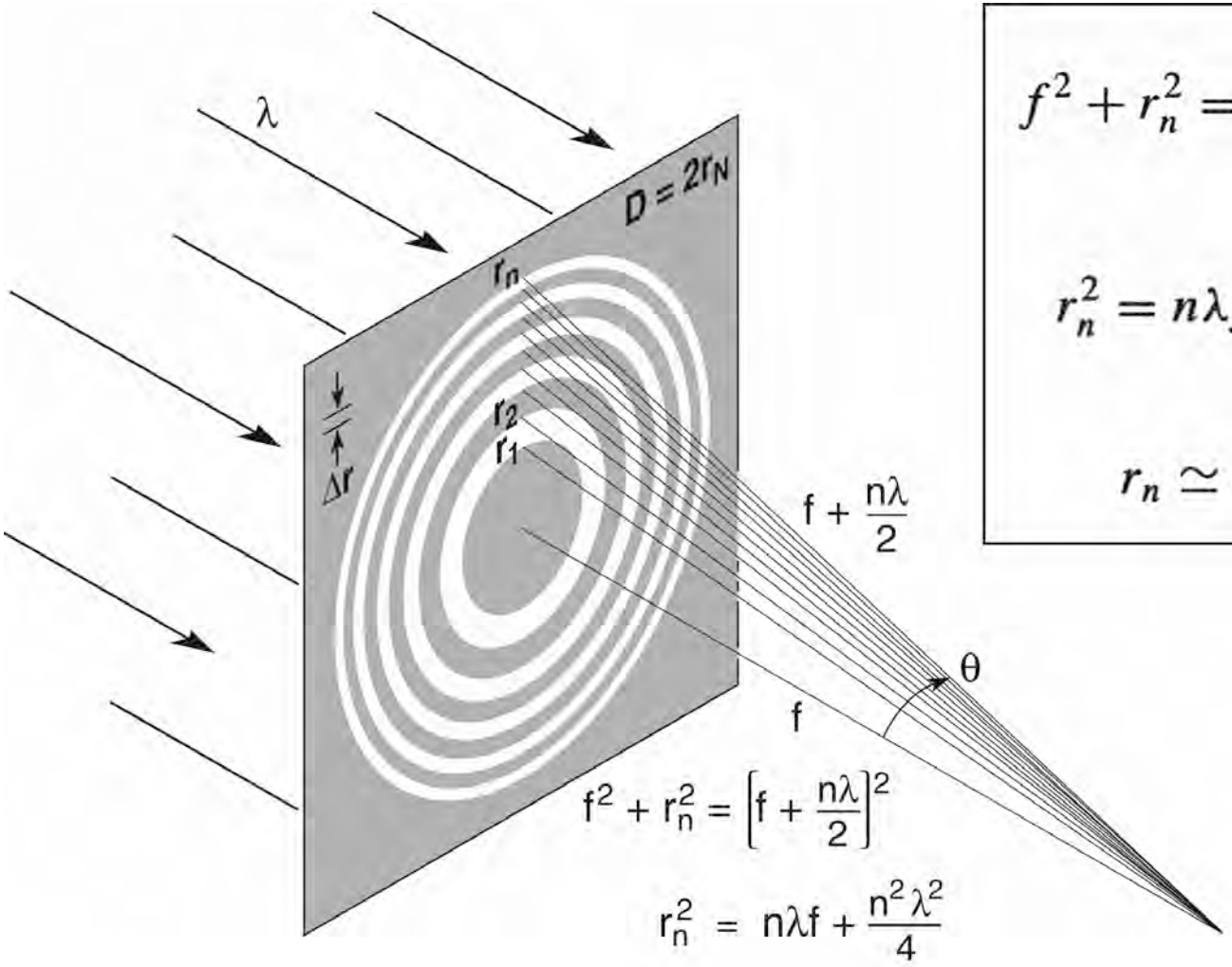

$$f^2 + r_n^2 = \left(f + \frac{n\lambda}{2}\right)^2 \qquad (9.8)$$

$$r_n^2 = n\lambda f + \frac{n^2\lambda^2}{4} \qquad (9.9)$$

$$r_n \simeq \sqrt{n\lambda f} \qquad (9.10)$$

Ch09_F05VG.ai

A Fresnel zone plate lens used as a diffractive lens for point to point imaging

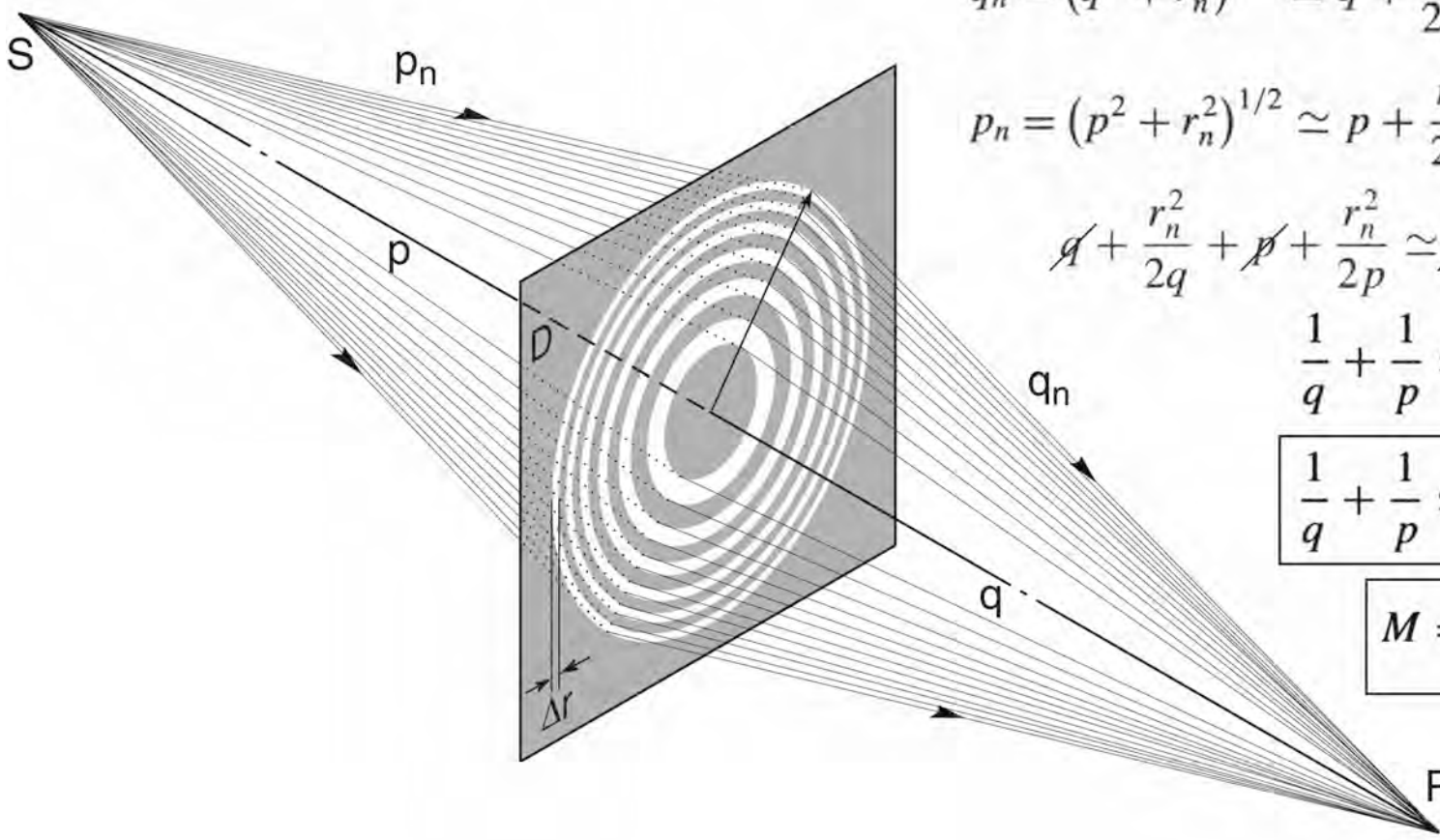

$$q_n + p_n = q + p + \frac{n\lambda}{2}$$

$$q_n = (q^2 + r_n^2)^{1/2} \simeq q + \frac{r_n^2}{2q}$$

$$p_n = (p^2 + r_n^2)^{1/2} \simeq p + \frac{r_n^2}{2p}$$

$$\cancel{q} + \frac{r_n^2}{2q} + \cancel{p} + \frac{r_n^2}{2p} \simeq \cancel{q} + \cancel{p} + \frac{n\lambda}{2}$$

$$\frac{1}{q} + \frac{1}{p} \simeq \frac{n\lambda}{r_n^2}$$

$$\boxed{\frac{1}{q} + \frac{1}{p} \simeq \frac{1}{f}} \quad (9.17)$$

$$\boxed{M = \frac{p}{q}} \quad (9.18)$$

Ch09_F02_modif.VG.ai

Depth of focus and spectral bandwidth

$$\Delta z = \pm \frac{1}{2} \frac{\lambda}{(\mathrm{NA})^2} \qquad (9.50)$$

$$\Delta z = \pm 2F^{\#2}\lambda = \pm 2(\Delta r)^2/\lambda \qquad (9.51)$$

$$\frac{\Delta\lambda}{\lambda} \leq \frac{1}{N} \qquad (9.52)$$

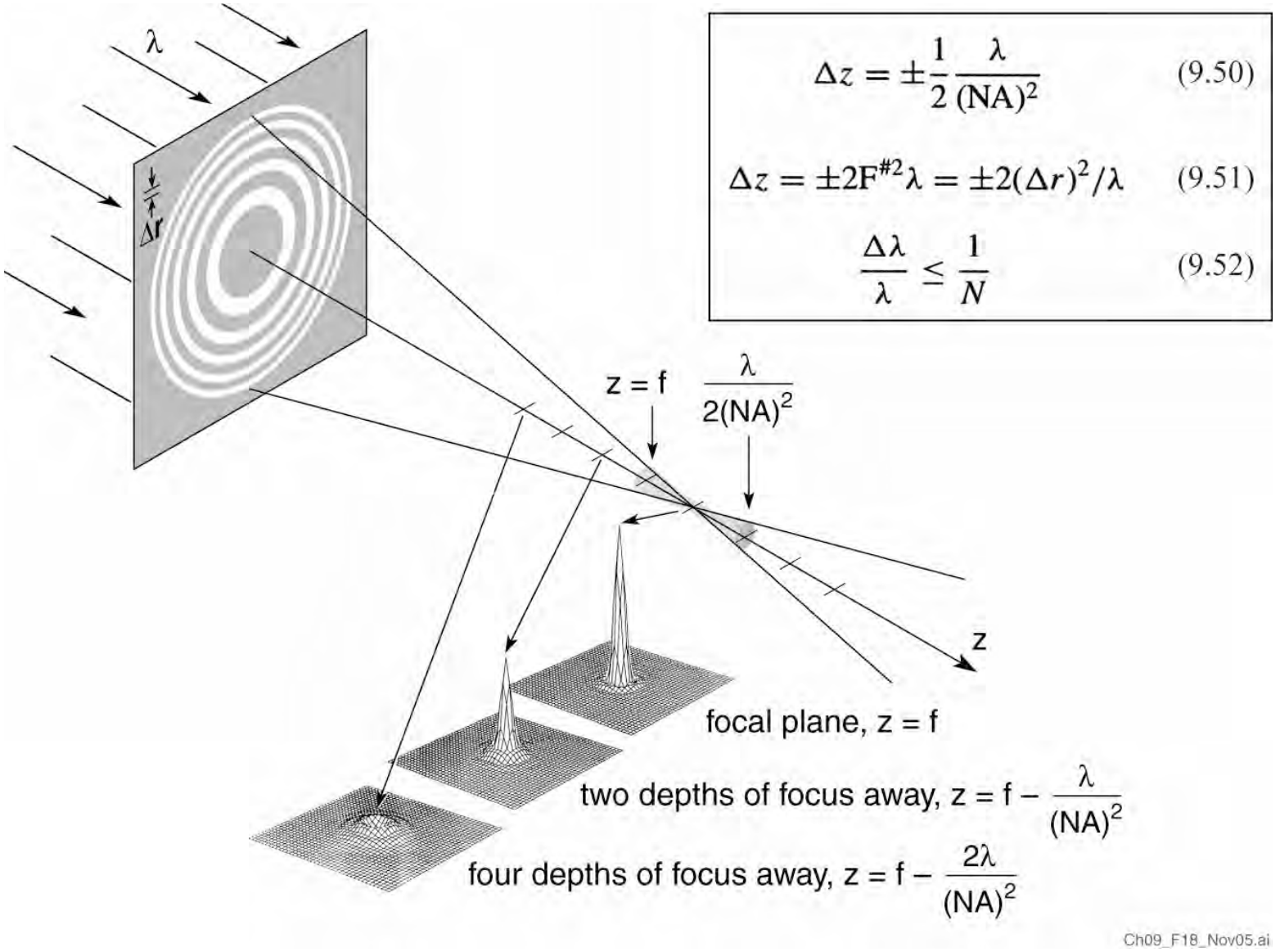

A Fresnel one plate lens used for x-ray microscopy

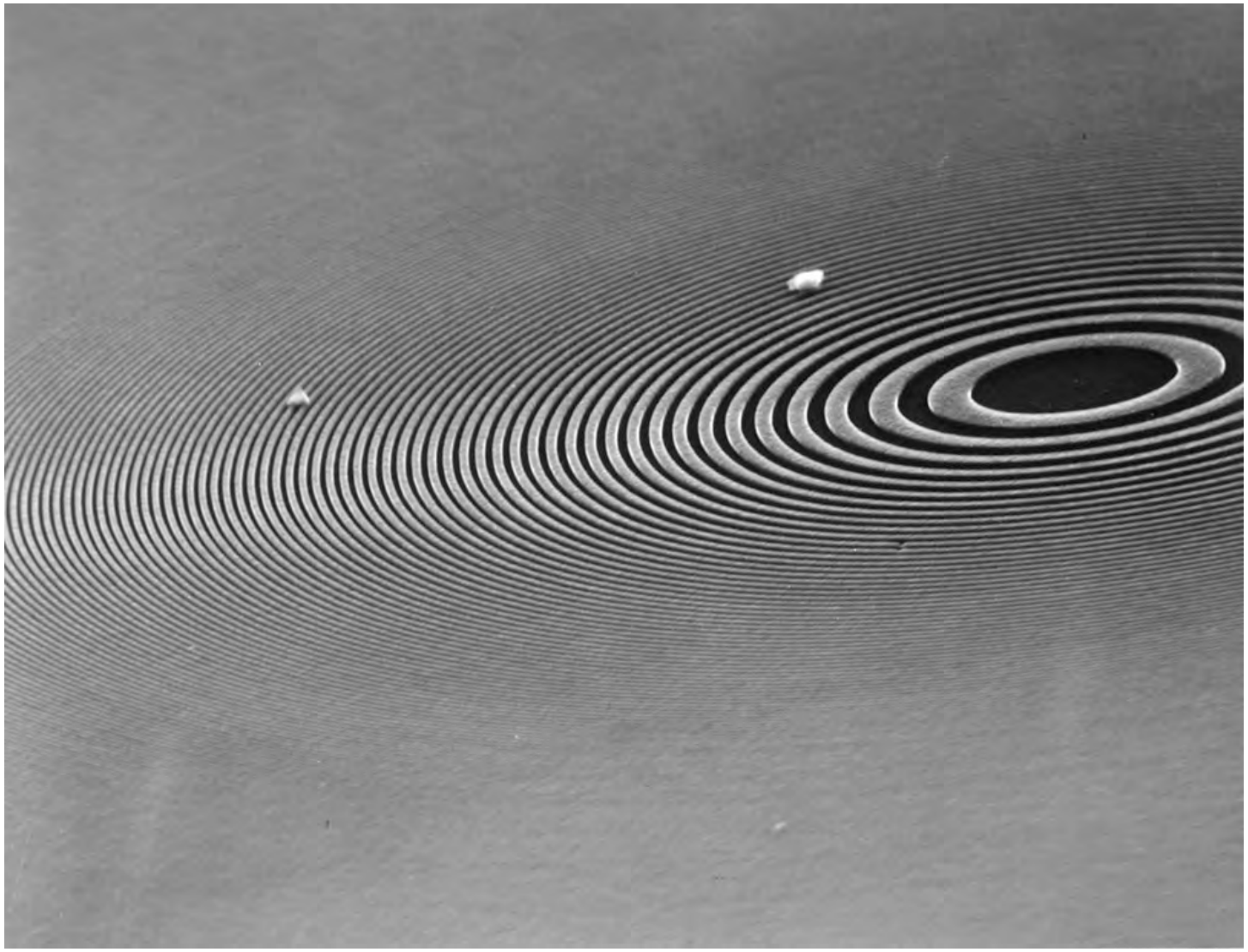

Courtesy of E. Anderson (LBNL)

Zone plate lens with 15 nm outer zone width

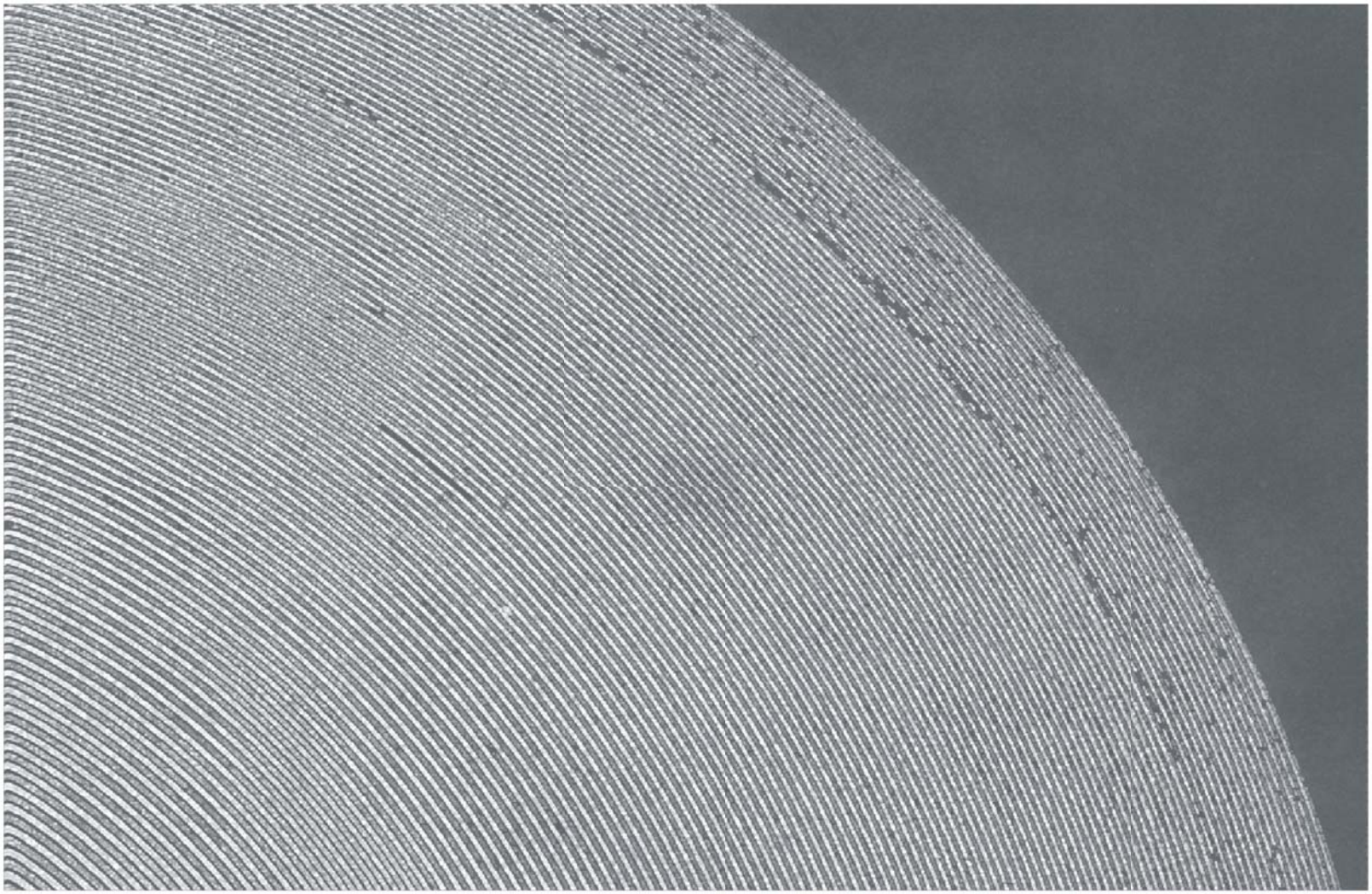

W. Chao et al., Nature, 30 June 2005

The Nanowriter: high resolution electron beam writing with high placement accuracy

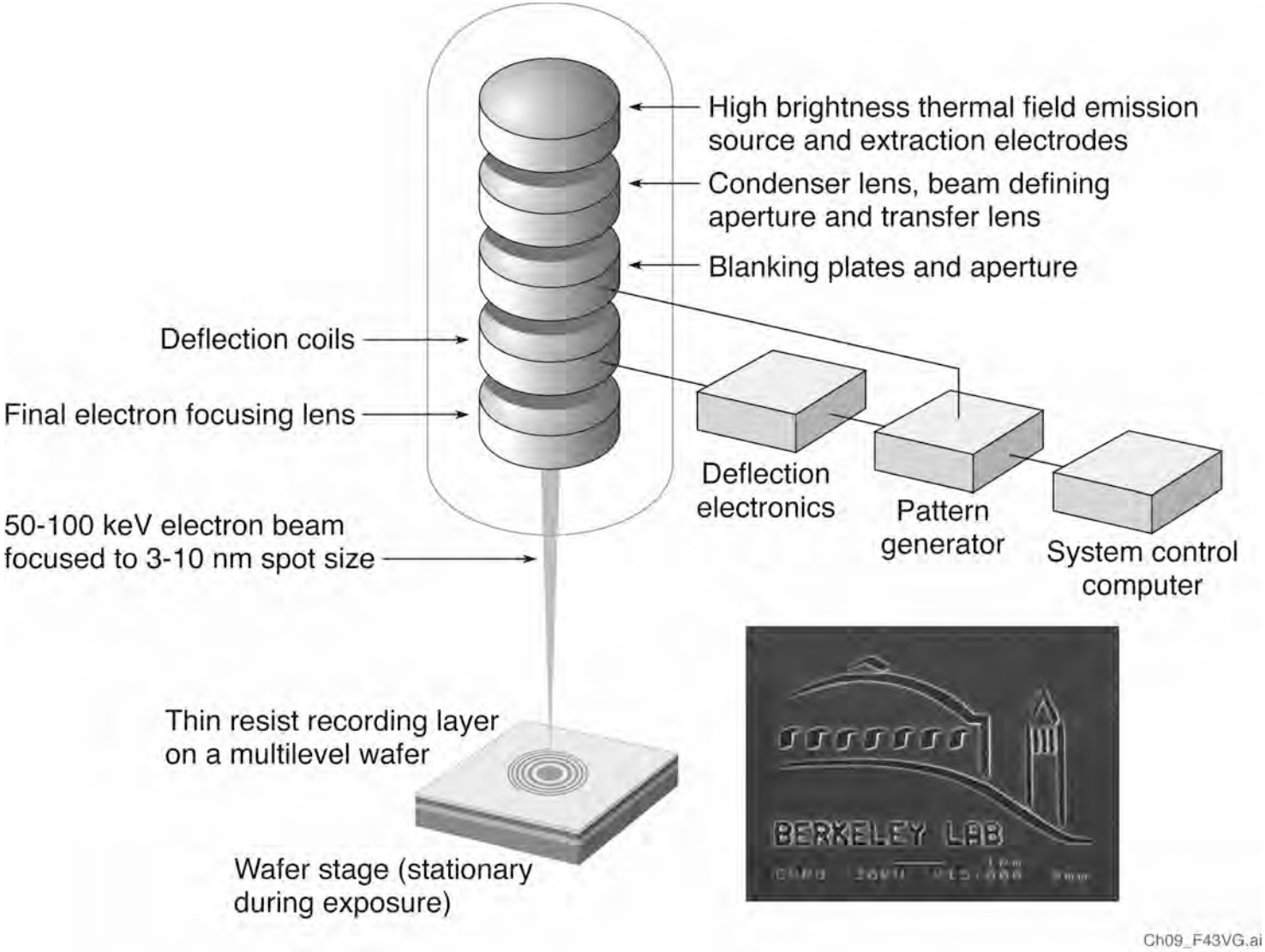

Courtesy of E. Anderson (LBNL)

Zone plate diffractive focusing for higher orders

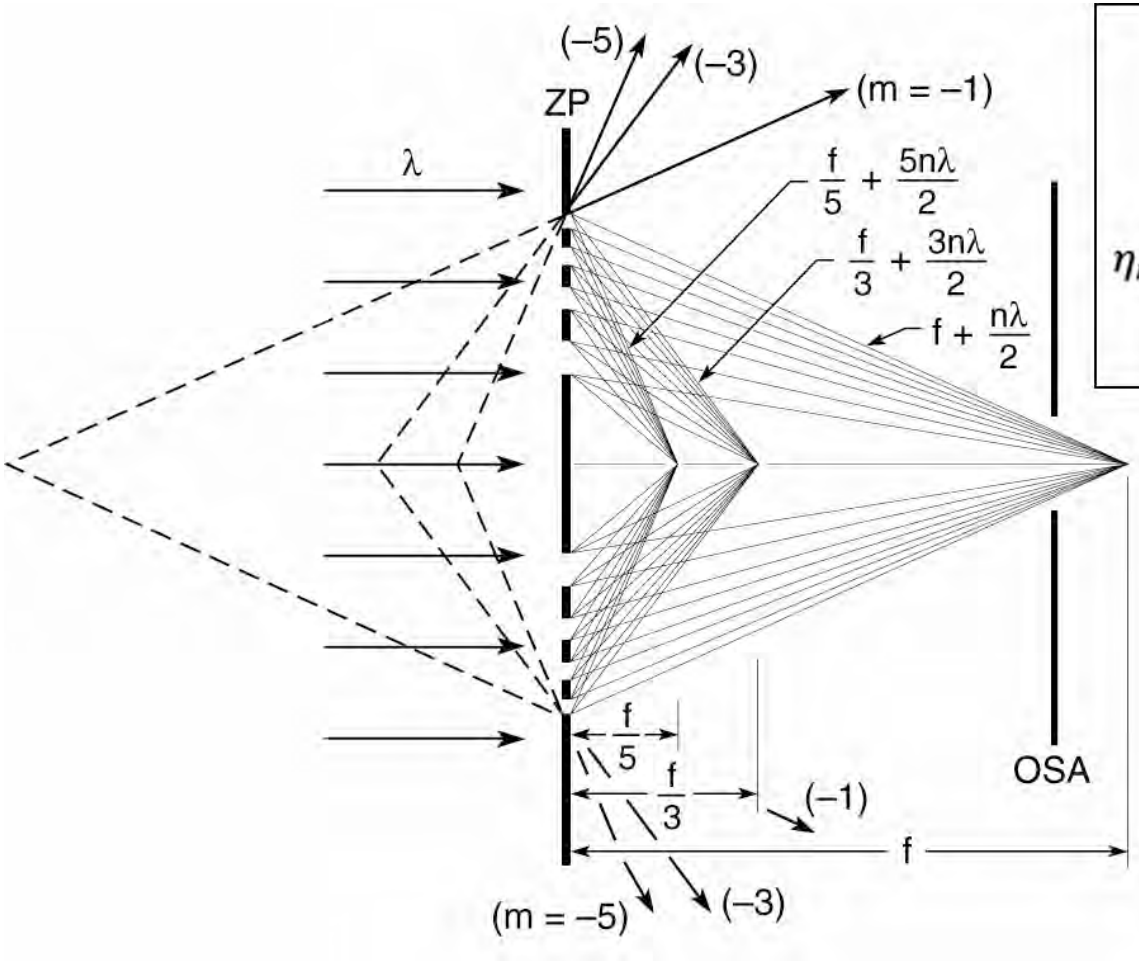

$$r_n^2 \simeq mn\lambda f_m \qquad (9.19)$$

$$\eta_m = \begin{cases} \frac{1}{4} & m = 0 \\ 1/m^2\pi^2 & m \text{ odd} \\ 0 & m \text{ even} \end{cases} \qquad (9.24)$$

$$f_m = \frac{1}{m}\,\frac{r_N^2}{N\lambda}$$

$$f_m = \frac{1}{m}\,f_1$$

Ch09_F08_Nov05.ai

High resolution zone plate microscope XM-1 at the ALS

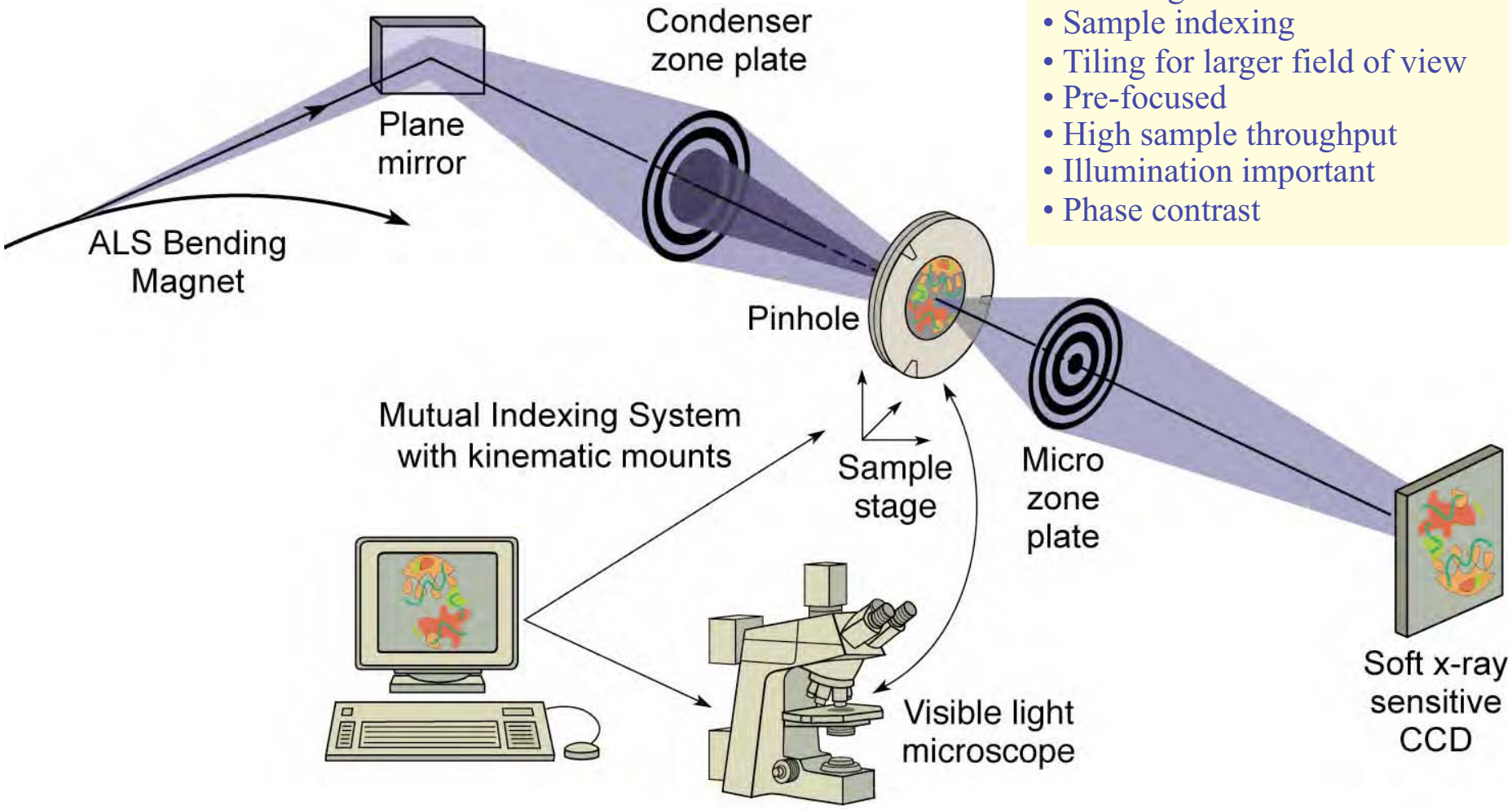

- Well engineered
- Sample indexing
- Tiling for larger field of view
- Pre-focused
- High sample throughput
- Illumination important
- Phase contrast

HiResZPMicrXM1Biology_Apr08.ai

Applications of soft x-ray microscopy

Magnetic Recording Materials

100 nm lines & spaces

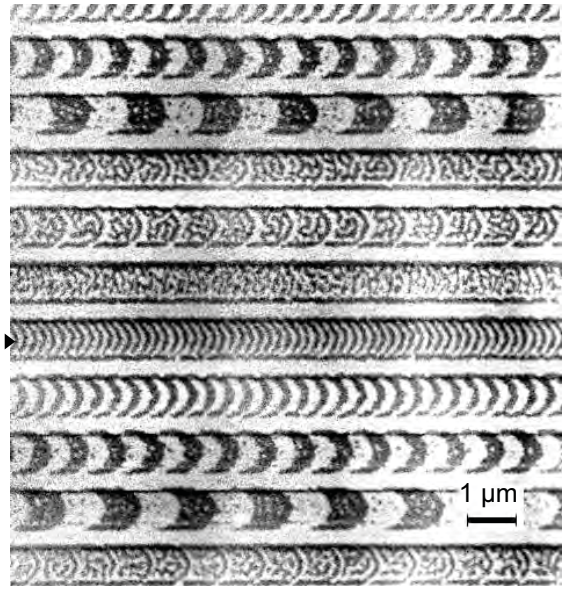

Fe L_3 @ 707.5 eV

FeTbCo Multilayer
with Al Capping Layer

Courtesy of P. Fischer (Max Planck)
and G. Denbeaux (CXRO/LBNL)

Cryo Microscopy for the Life Sciences

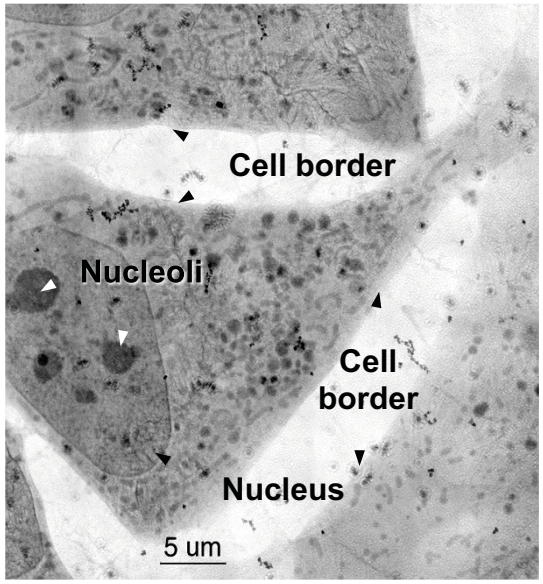

Cryo X-Ray Microscopy
of 3T3 Fibroblast Cells

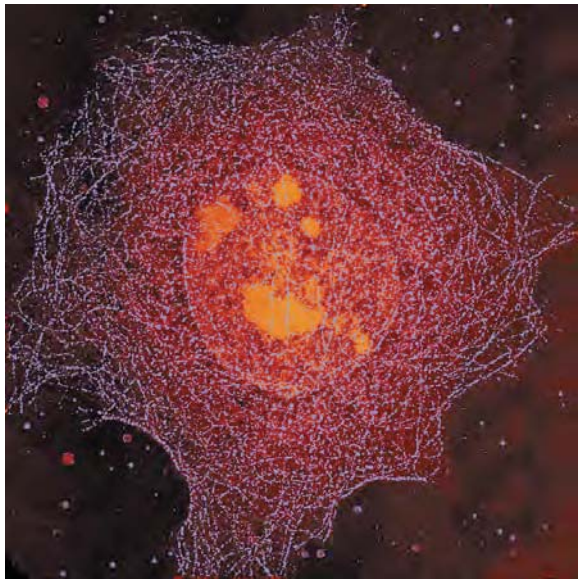

Protein Labeled
Microtubule Network

Courtesy of C. Larabell (UCSF)
and W. Meyer-Ilse (CXRO/LBNL)

Bio-nanotomography for 3D imaging of cells

Nanotomography of Cryogenic Fixed Cells

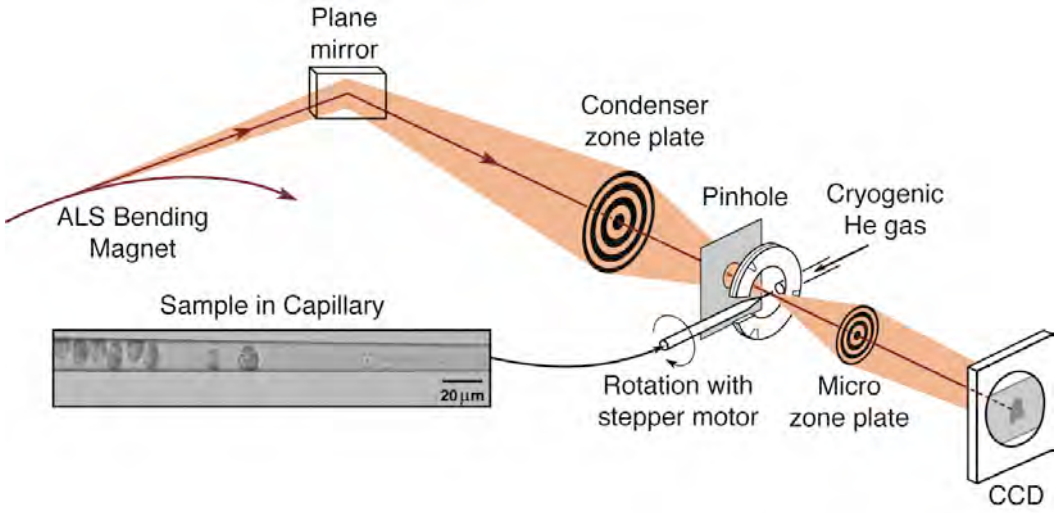

Courtesy of G. Schneider (BESSY)
Surf. Rev. Lett. 9, 177 (2002)

Soft X-Ray Nanotomography of a Yeast Cell

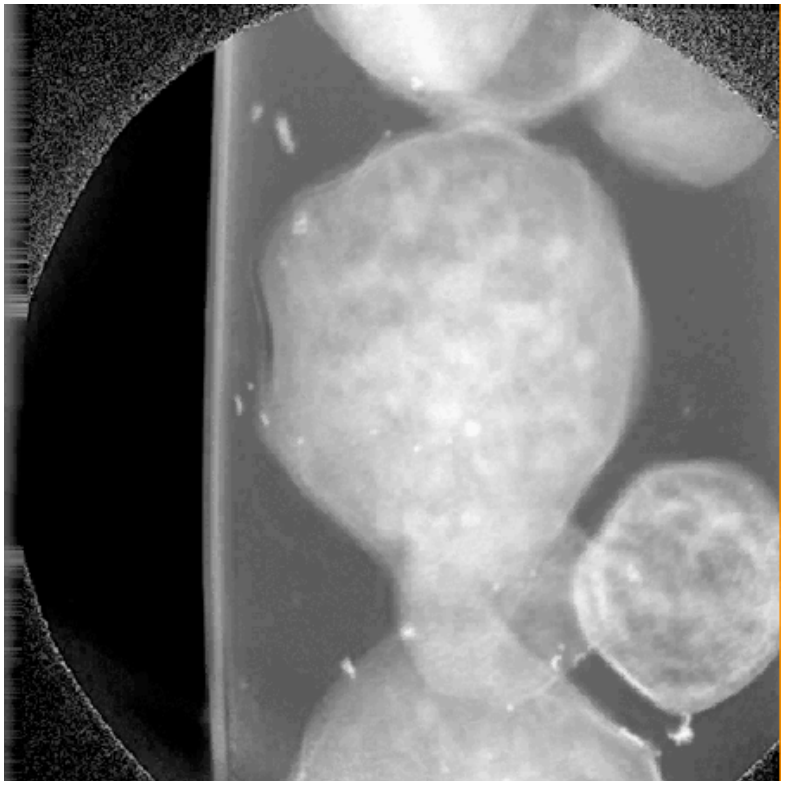

λ = 2.5 nm

Courtesy of C. Larabell (UCSF & LBNL) and M. LeGros (LBNL)

NCXT

Bio-nanotomography for 3D imaging of cells

Nanotomography of Cryogenic Fixed Cells

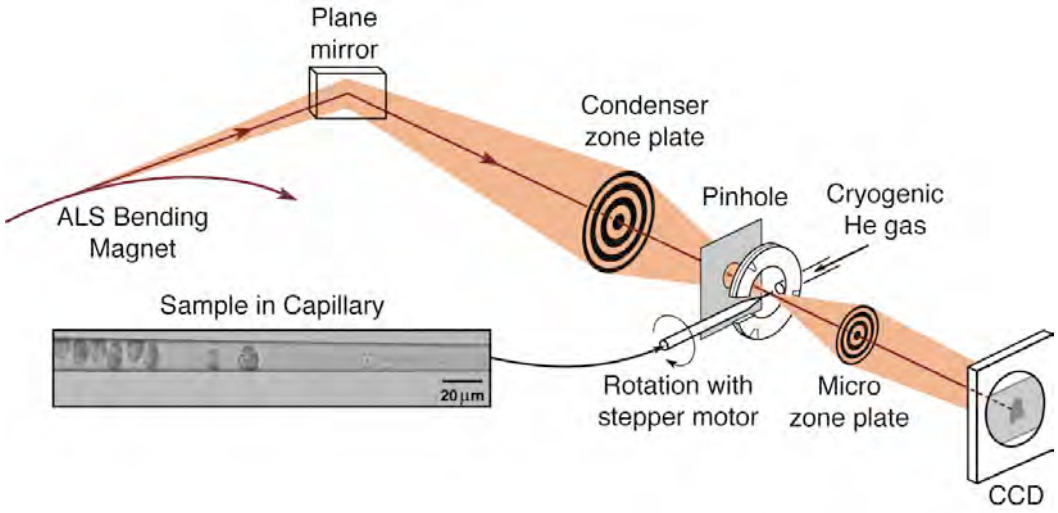

Soft X-Ray Nanotomography of a Yeast Cell

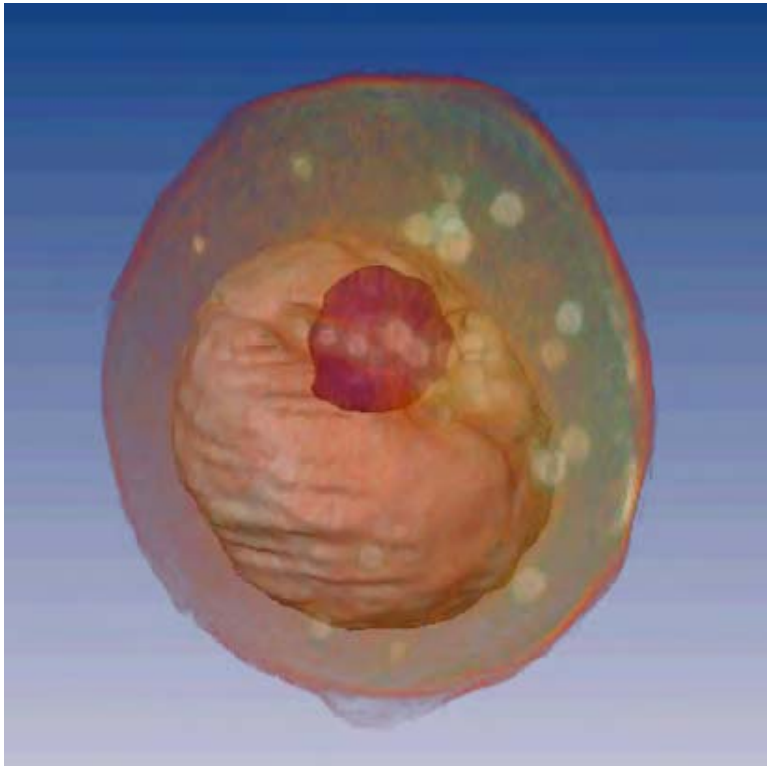

λ = 2.5 nm

C. Larabell and M. LeGros,
Molec. Bio. Cell 15, 957 (2004)

NCXT

Magnetic recording of nanomagnetic patterns to 15 nm spatial resolution

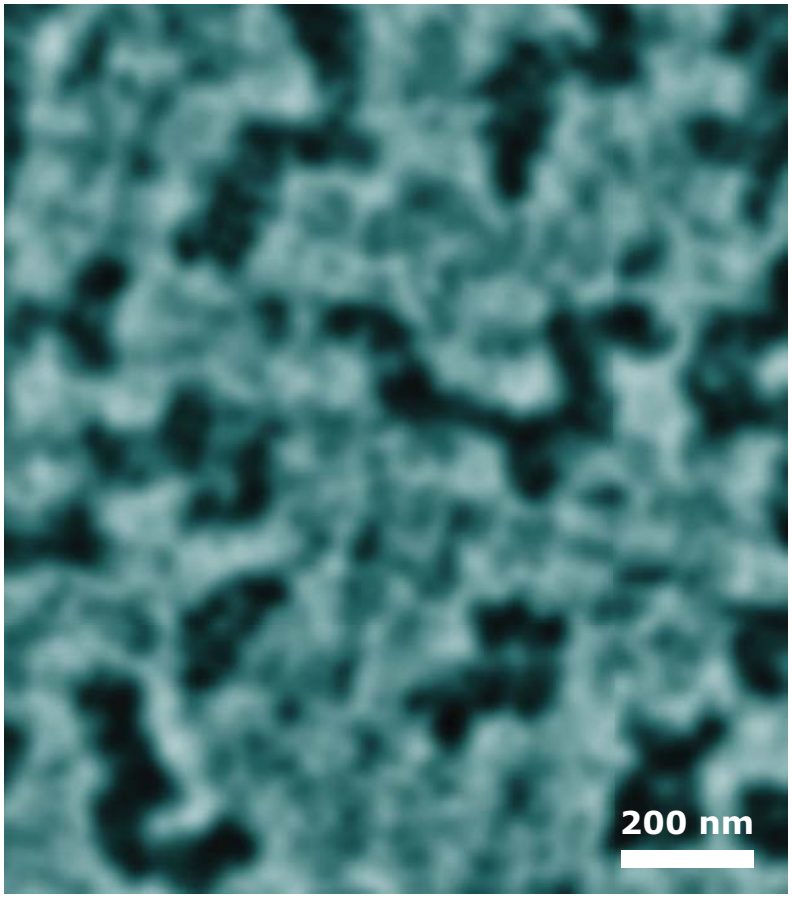

CoCrPt alloy
Co L_3-edge at 778 eV
(1.59 nm)

Courtesy of Peter Fischer (LBNL)

P. Fischer et al., *Mat. Today* 9, 26 (2006).

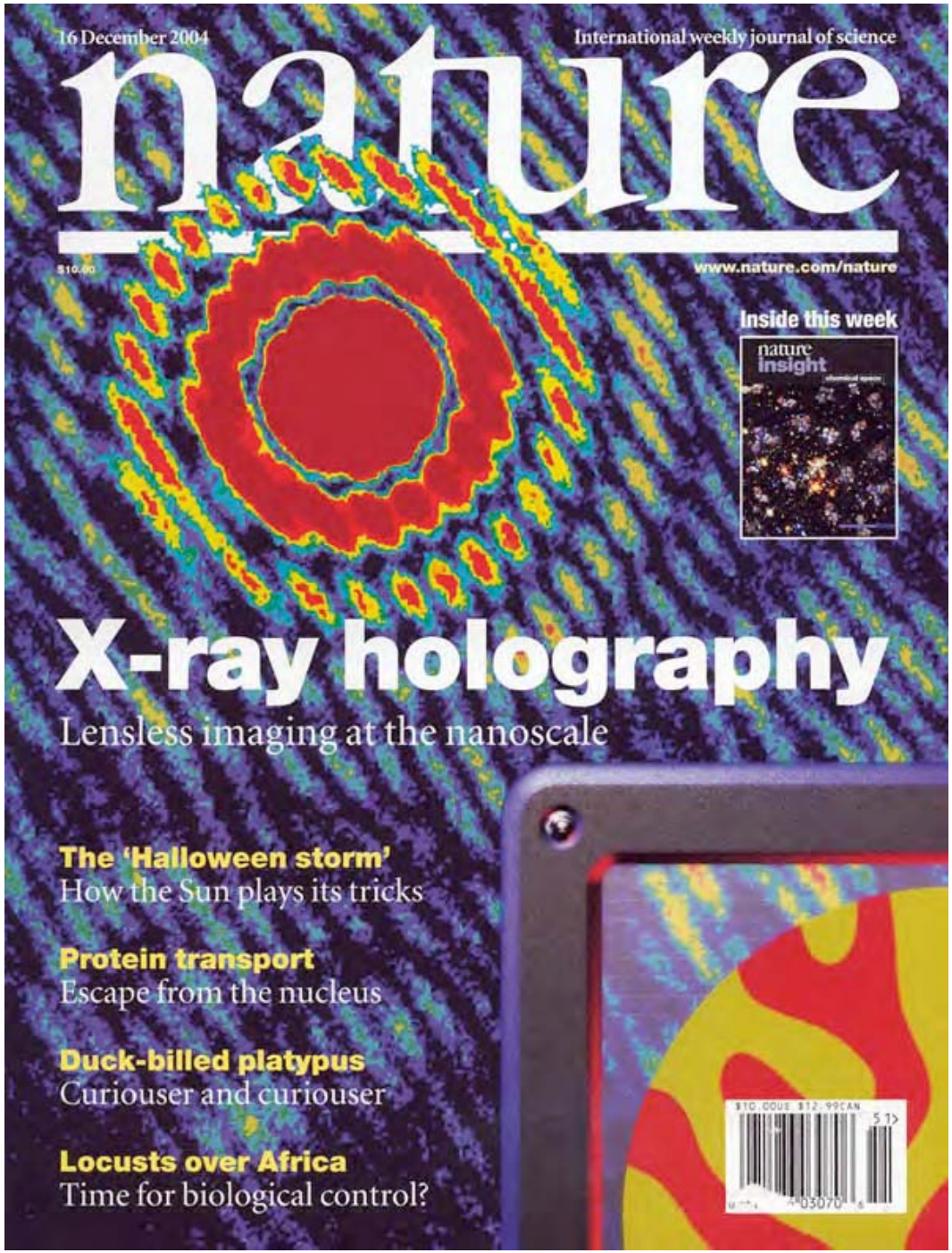
16 December 2004
International weekly journal of science
nature
www.nature.com/nature
Inside this week
nature insight
X-ray holography
Lensless imaging at the nanoscale
The 'Halloween storm'
How the Sun plays its tricks
Protein transport
Escape from the nucleus
Duck-billed platypus
Curiouser and curiouser
Locusts over Africa
Time for biological control?

Interference and reconstruction

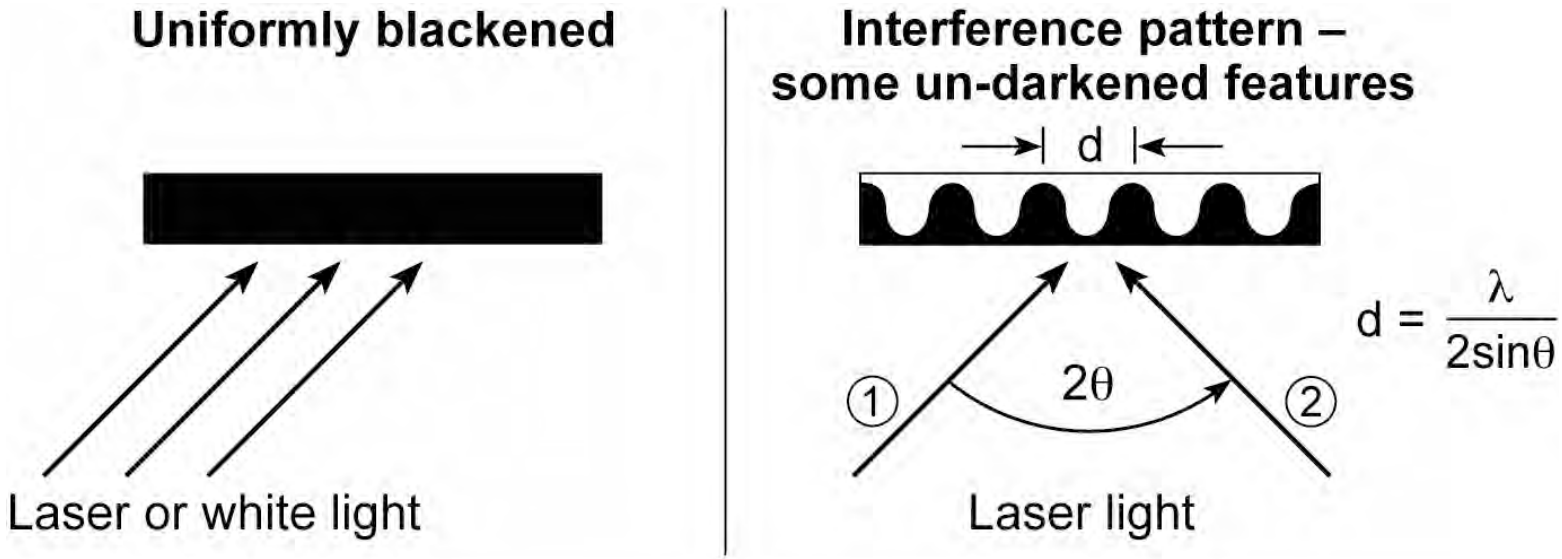

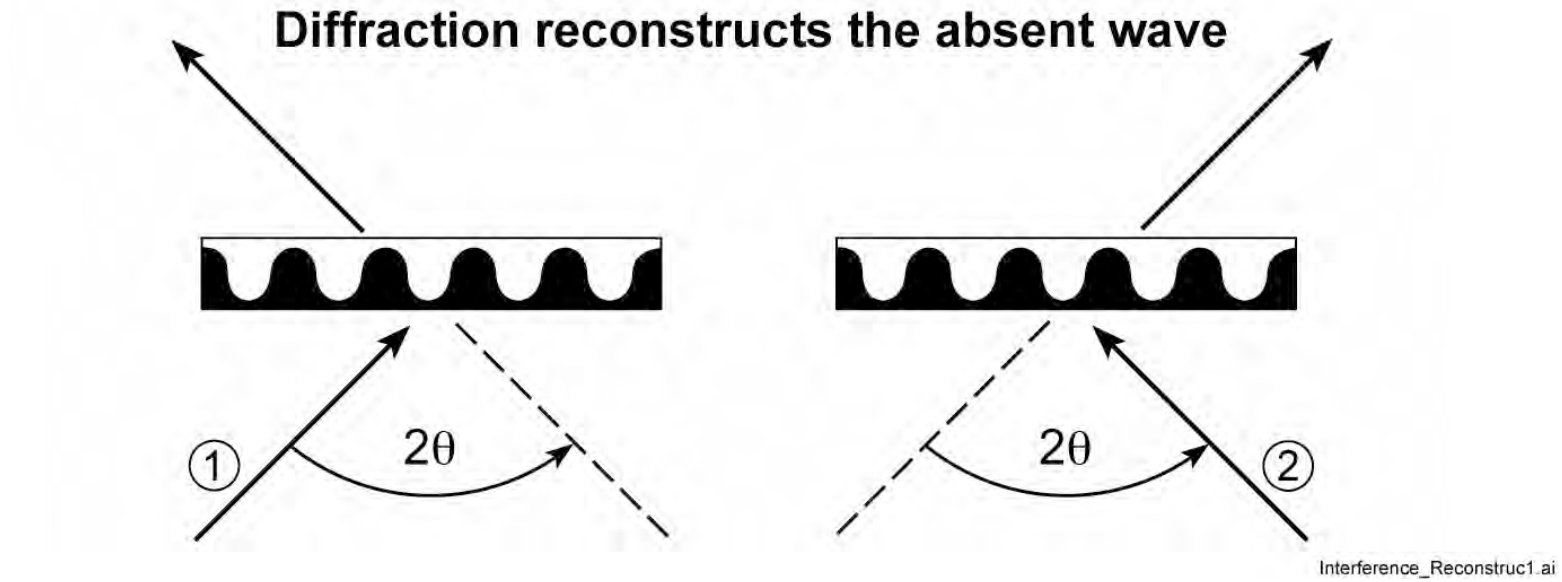

Interference_Reconstruc1.ai

Interference and reconstruction (continued)

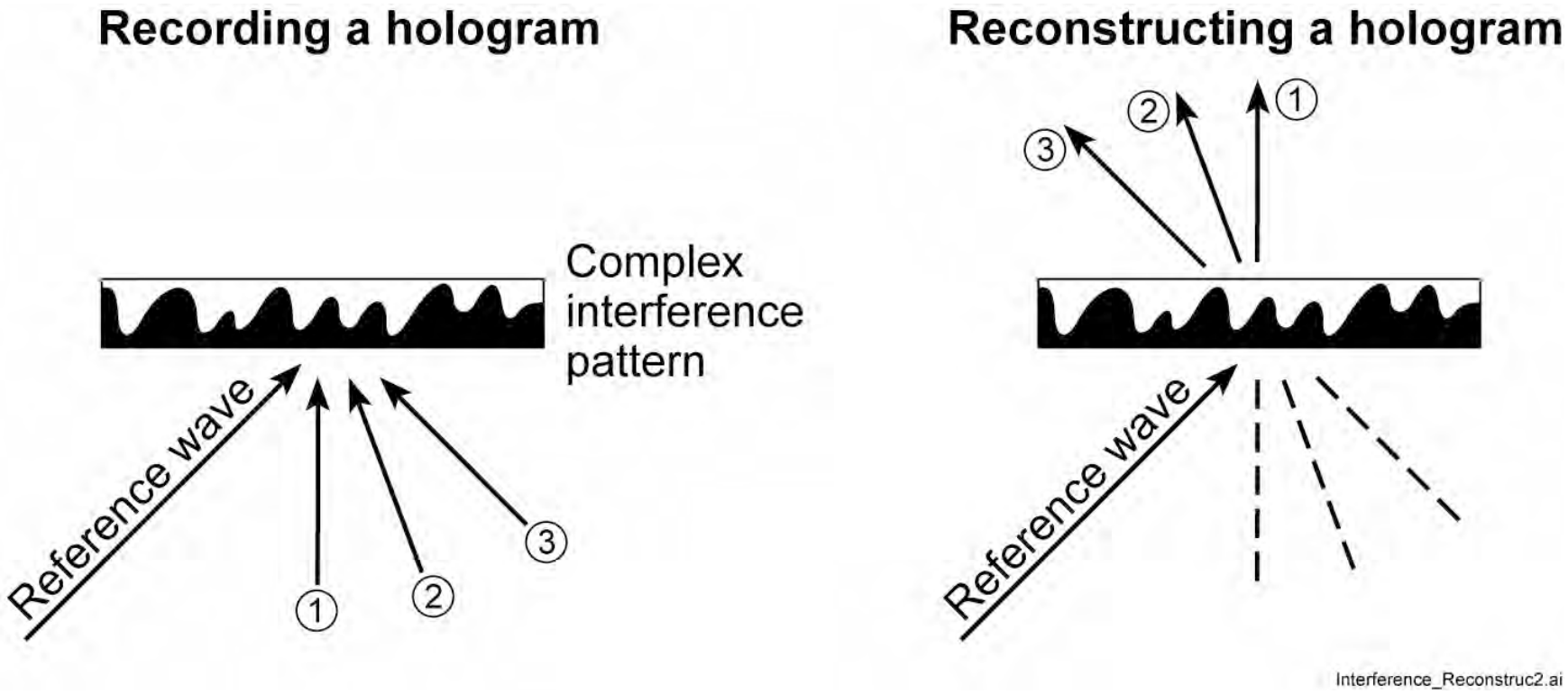

Holographic recording of a 3-D object

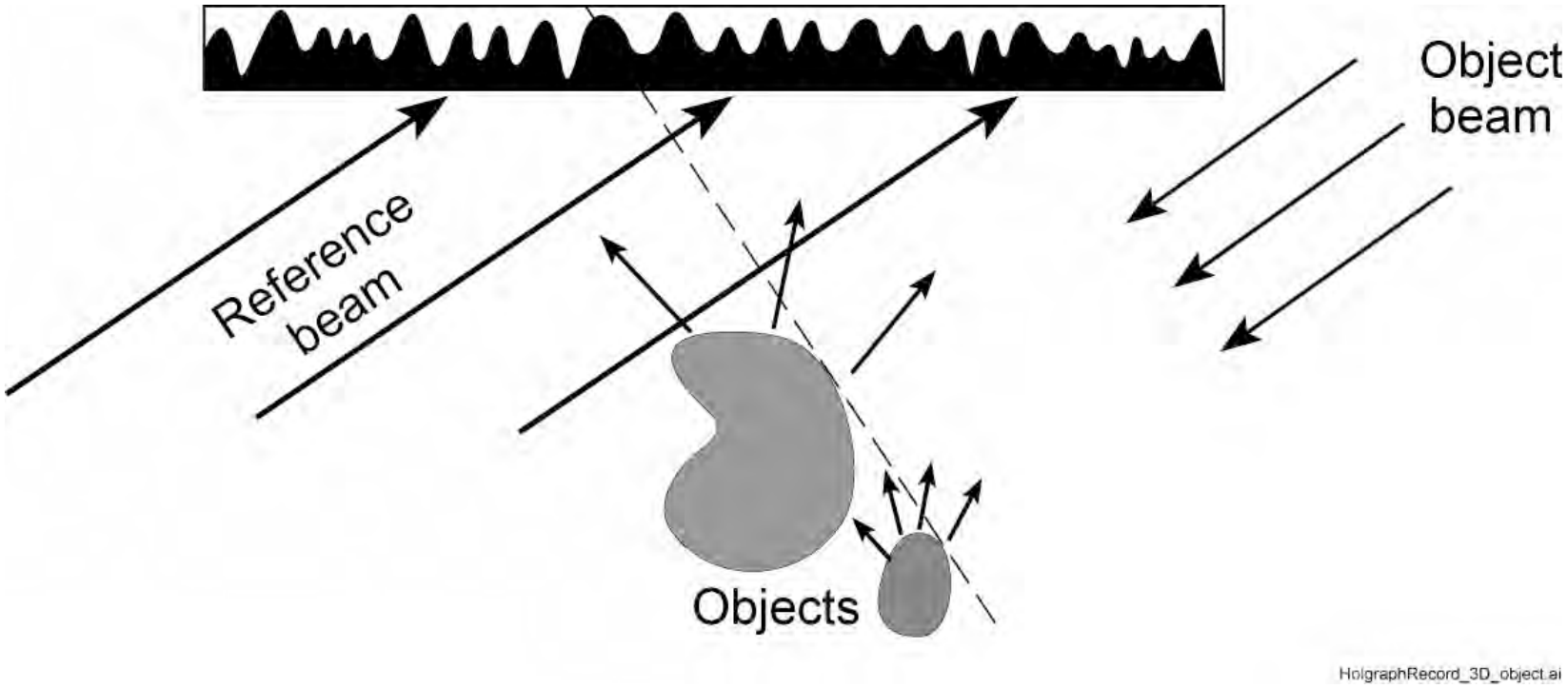

Holographic reconstruction (viewing)

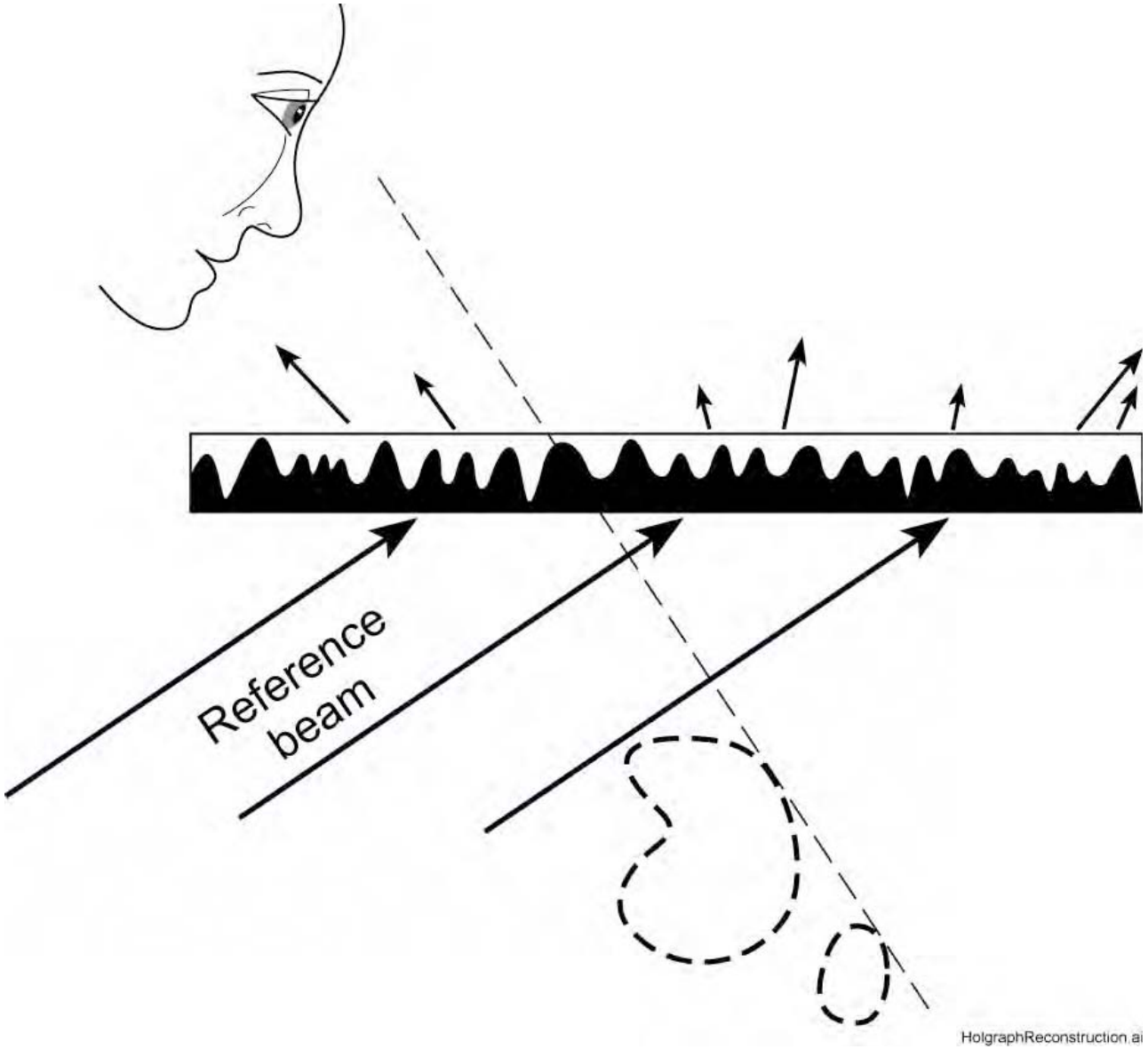

Lensless imaging of magnetic nanostructures by x-ray spectro-holography

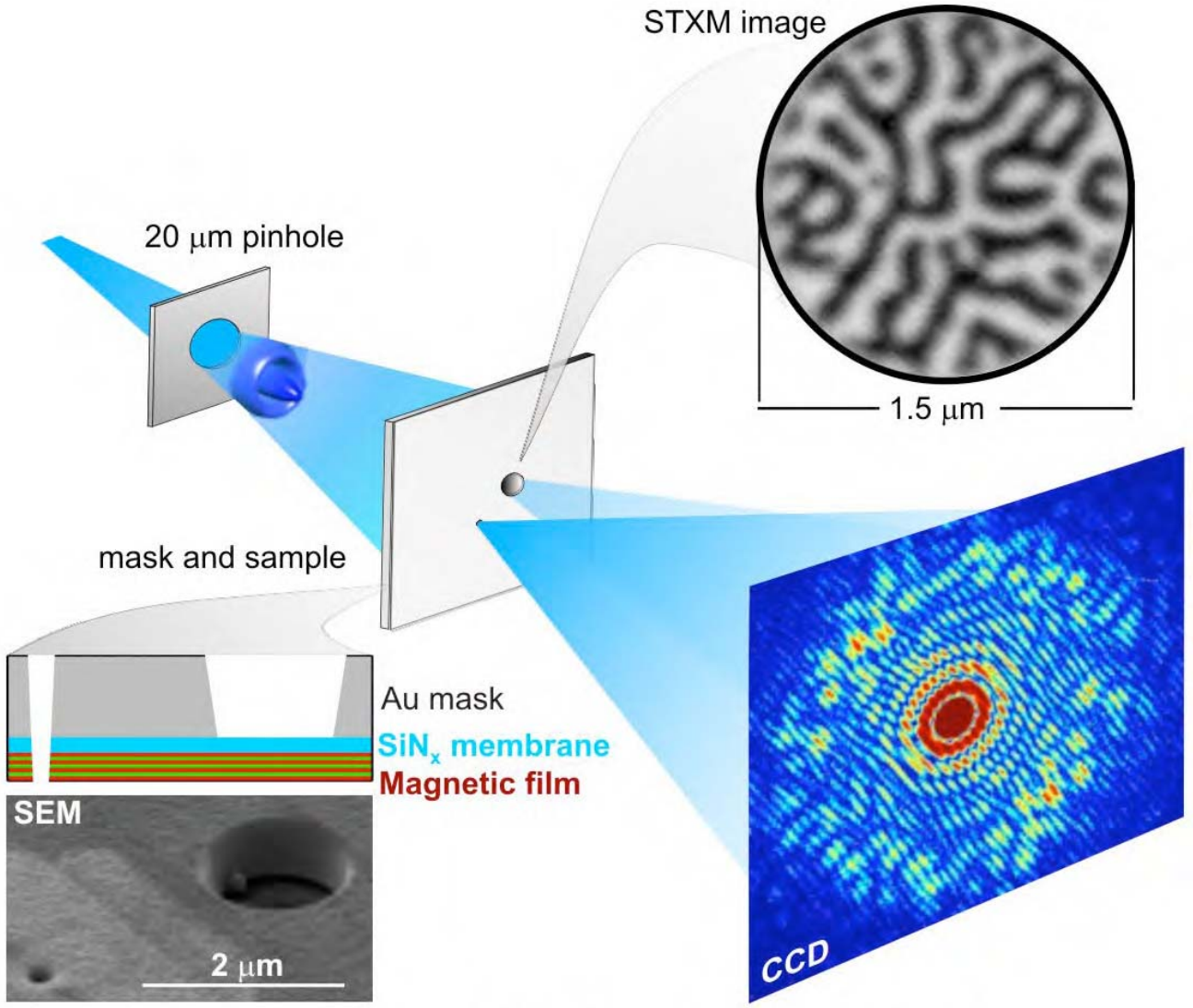

S. Eisebitt, J. Lüning, W.F. Schlotter, M. Lörgen, O. Hellwig, W. Eberhardt & J. Stöhr / *Nature*, 16 Dec 2004

LenslessImagingF1.ai